

2357-8

Innovations in Strongly Correlated Electronic Systems: School and Workshop

6 - 17 August 2012

Nematic transition and antiferromagnetic quantum critical point in BaFe₂(As_{1-x}P_x)₂

Takasada SHIBAUCHI
Kyoto University, Department of Physics
Kyoto
JAPAN

Nematic transition and antiferromagnetic quantum critical point in $\text{BaFe}_2(\text{As}_{1-x}\text{P}_x)_2$

Taka Shibauchi

Department of Physics, Kyoto University

1. Quantum phase transition lurking inside the superconducting dome

K. Hashimoto *et al.*, Science **336**, 1554 (2012).

2. Nematic transition above the dome

S. Kasahara *et al.*, Nature **486**, 382 (2012).

3. Summary – A renewed phase diagram



Collaborators

Transport properties
Penetration depth
Thermal conductivity
dHvA
Magnetic torque
Crystal growth

S. Kasahara
K. Hashimoto
Y. Mizumami
H. Shishido
T. Terashima
Y. Matsuda

Band calc.
H. Ikeda
NMR
T. Iye
K. Ishida



Kyoto Univ. Japan

Penetration depth, dHvA

A. Serafin

P. Walmsley

A. Carrington

Univ. of Bristol, UK



dHvA

A.I. Coldea

Univ. of Oxford, UK

Penetration depth

K. Cho

M. Tanatar

R. Prozorov

Ames, USA



N. Salovich

R. W. Giannetta



Univ. of Illinois at Urbana-Champaign, USA

Synchrotron X-ray

K. Sugimoto

SPring-8,

T. Fukuda

JAEA,

SPring-8, Japan



Theory (Nematic)

A. Nevidomskyy

Rice Univ. , USA



Ce₂PdIn₈ crystals

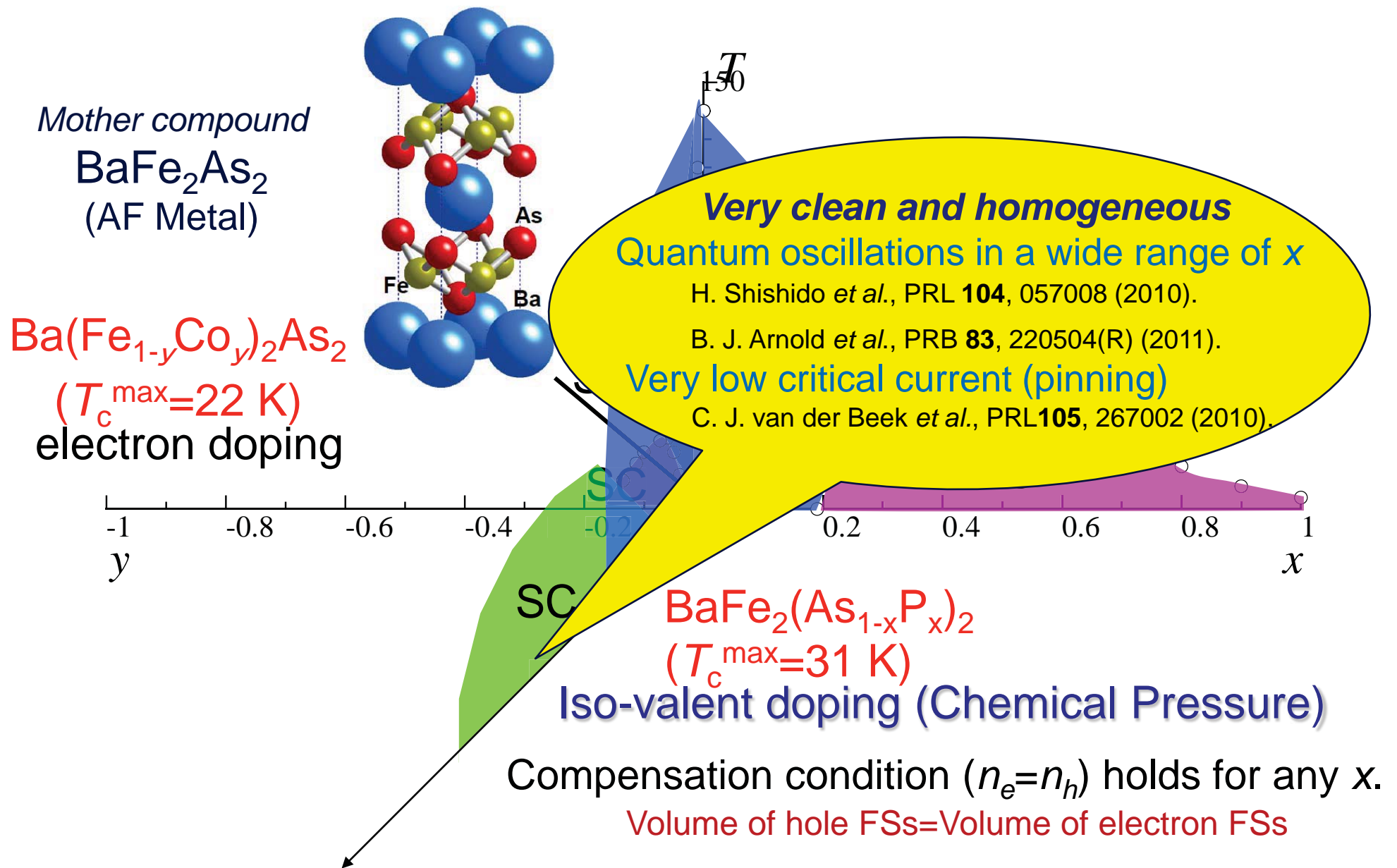
D. Gnida

D. Kaczorowski

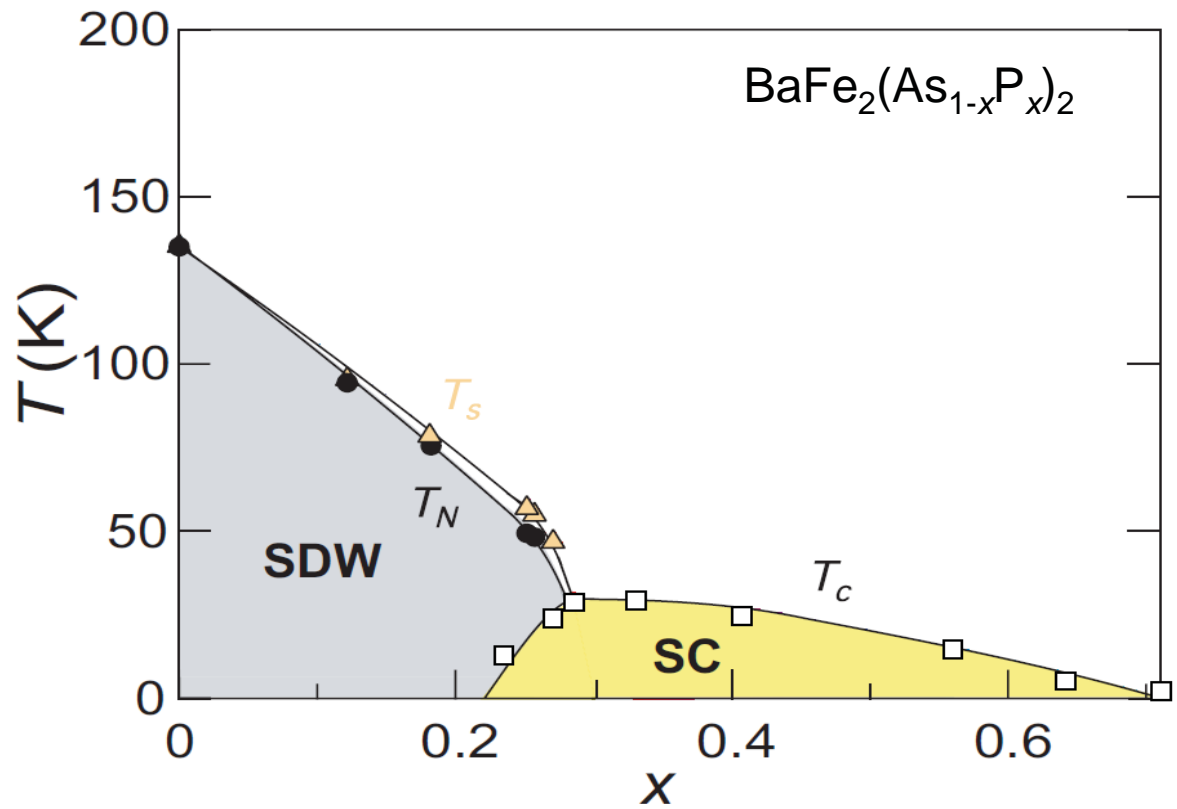
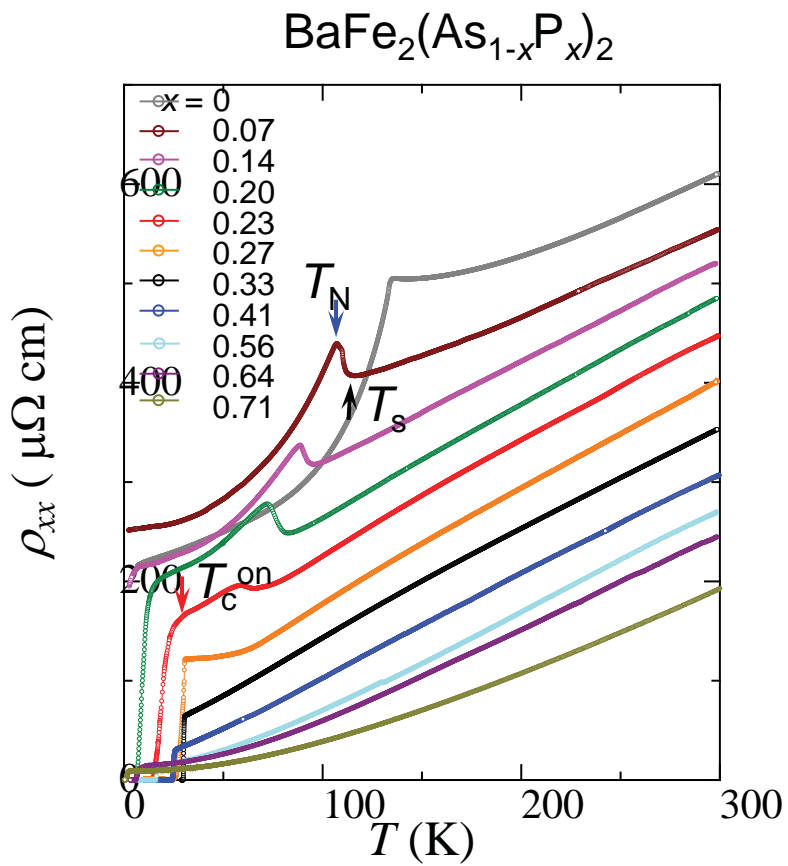


Polish Academy of Sciences, Poland

Superconductivity in BaFe_2As_2 systems

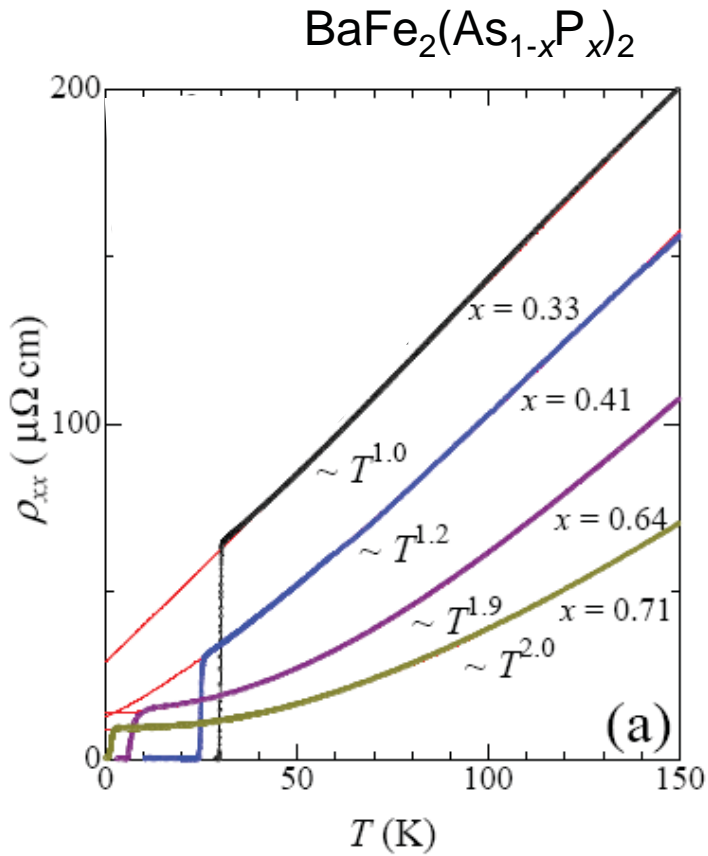


$\text{BaFe}_2(\text{As}_{1-x}\text{P}_x)_2$ is a clean system to study intrinsic properties



S. Kasahara, TS *et al.*, PRB **81**, 184519 (2010).

Doping evolution of transport properties

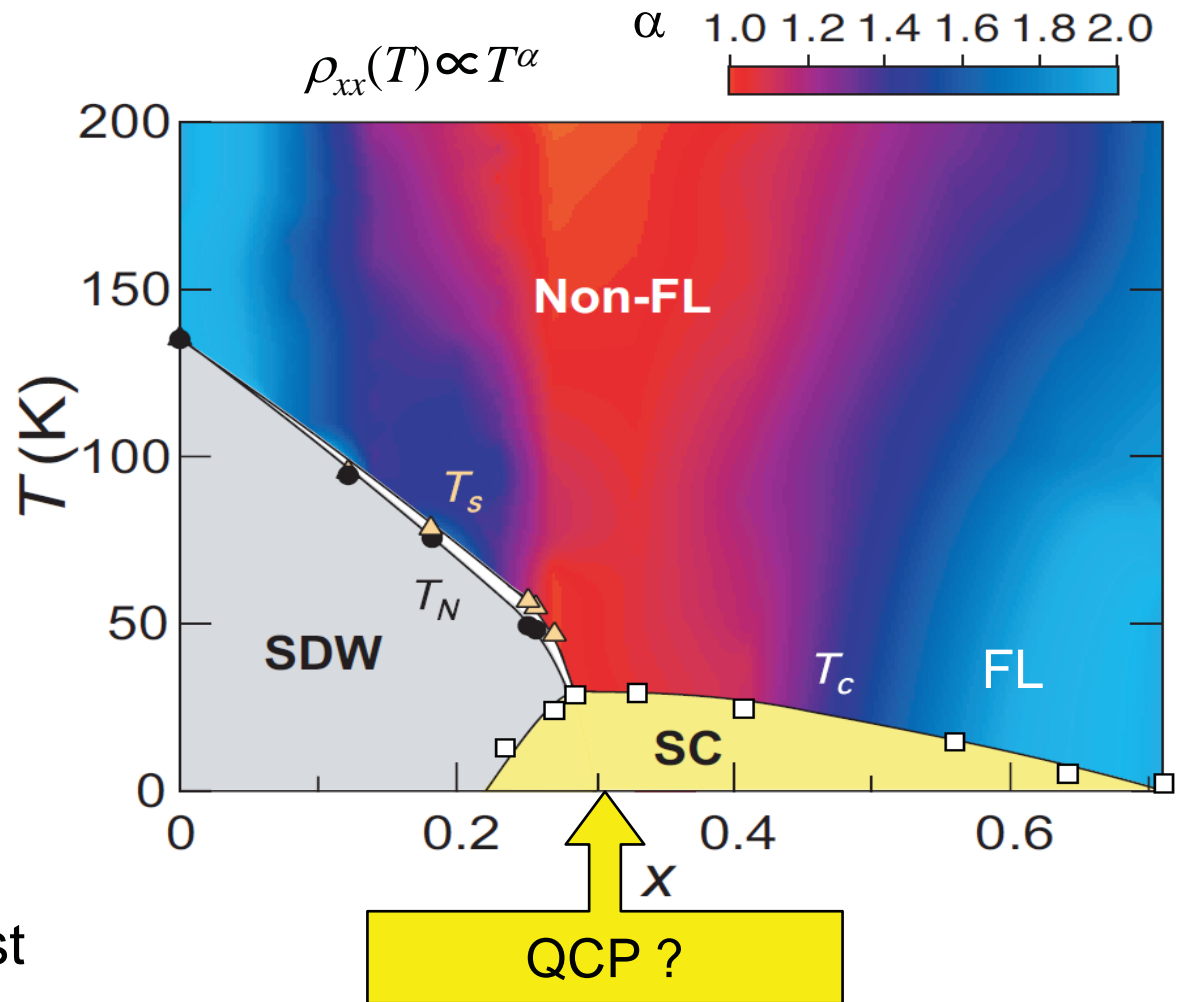


T -linear resistivity at $x=0.33$ just beyond the SDW end point

Hallmark of non-Fermi liquid

T^2 -dependence at $x=0.71$

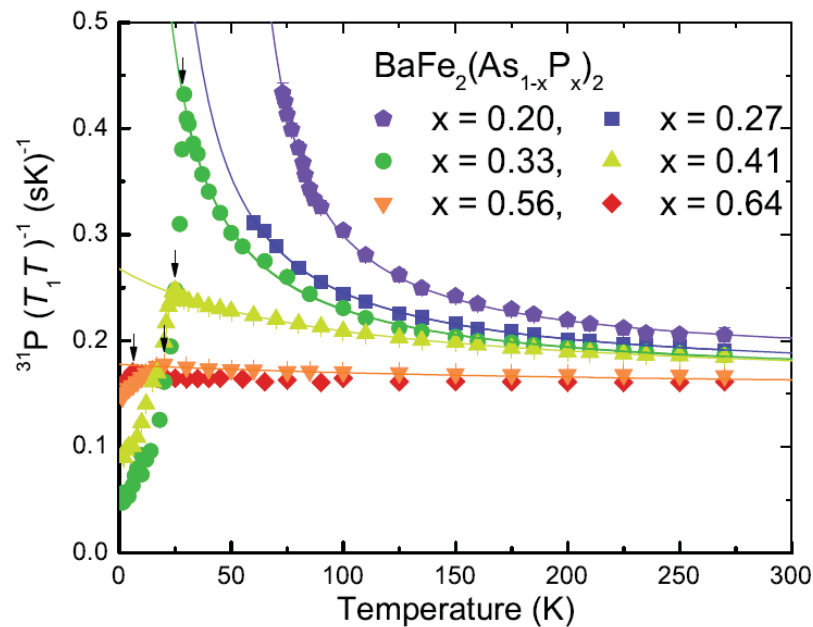
Fermi-liquid behavior



S. Kasahara, TS et al., PRB **81**, 184519 (2010).

See also J. Dai et al., PNAS (2009);
S. Sachdev and B. Keimer, Physics Today (2011).

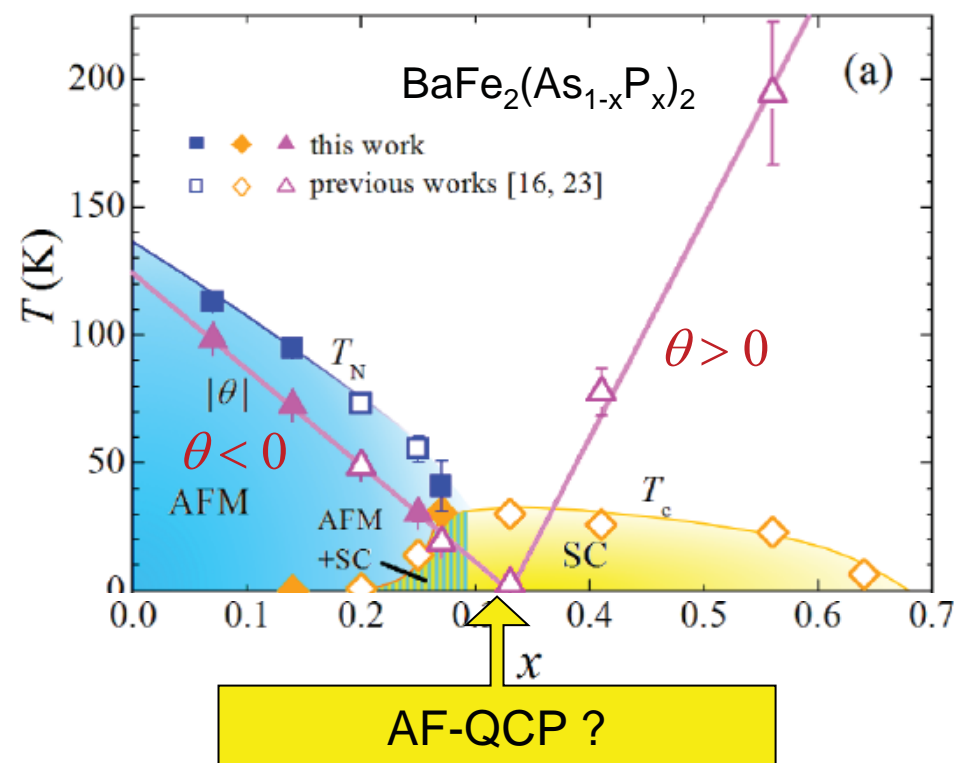
Doping evolution of the magnetic fluctuations (NMR)



$$\frac{1}{T_1 T} = a + \frac{b}{T + \theta}$$

θ : Weiss temperature

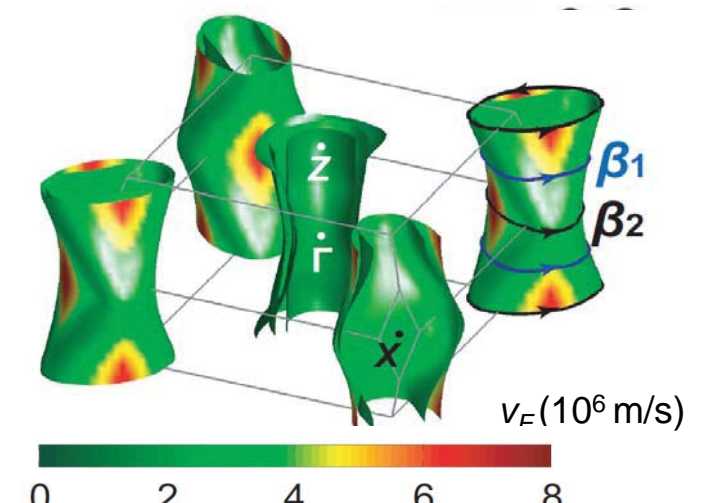
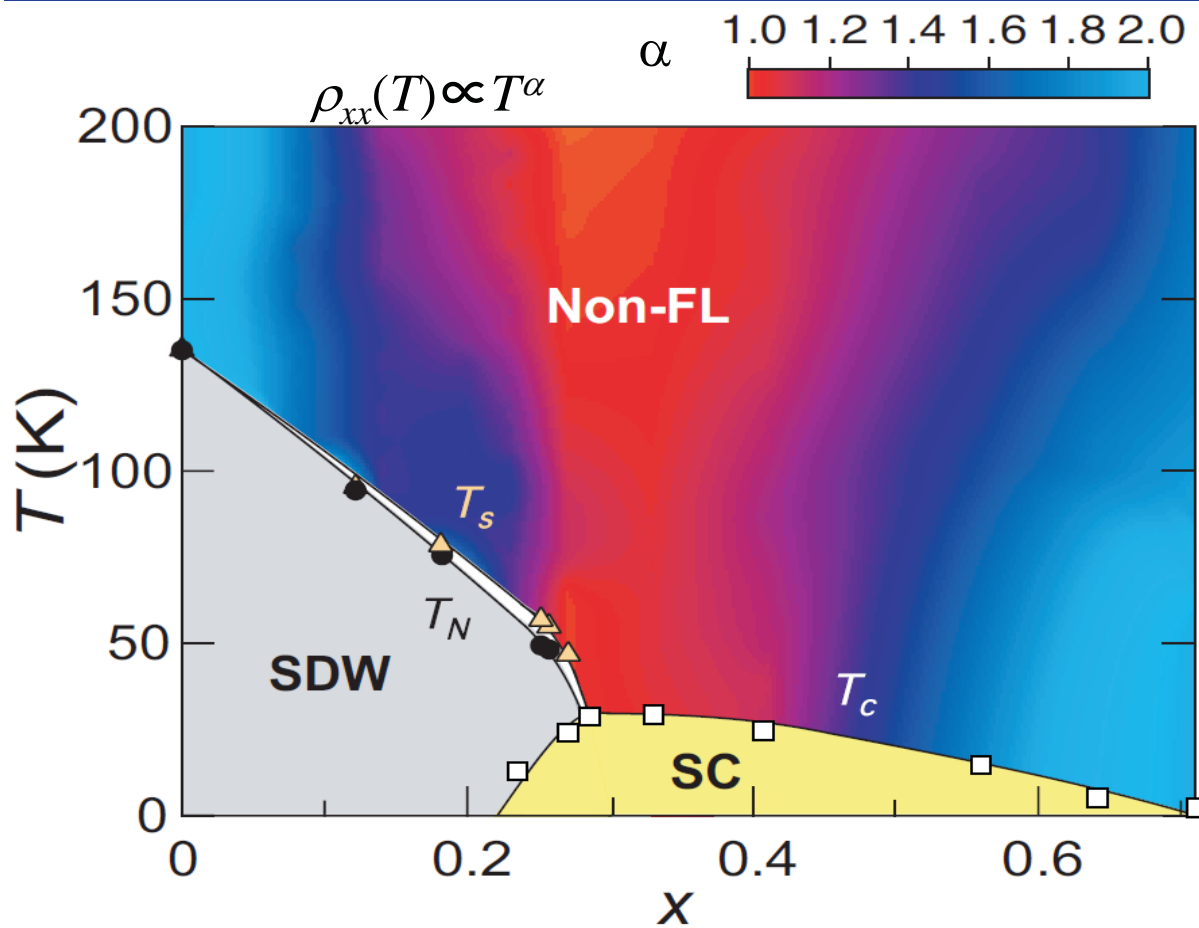
Y. Nakai *et al.* PRL (2010); T. Iye *et al.* PRB (2012)



θ goes to zero at $x \sim 0.3$

$\langle m \rangle$ goes to zero at $x \sim 0.3$

Doping evolution of electronic properties above T_c

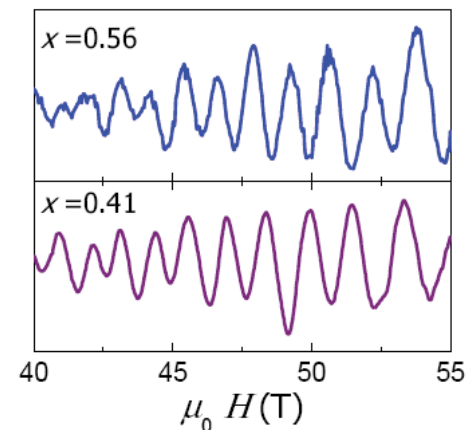


Effective mass m^*

Fermi temperature

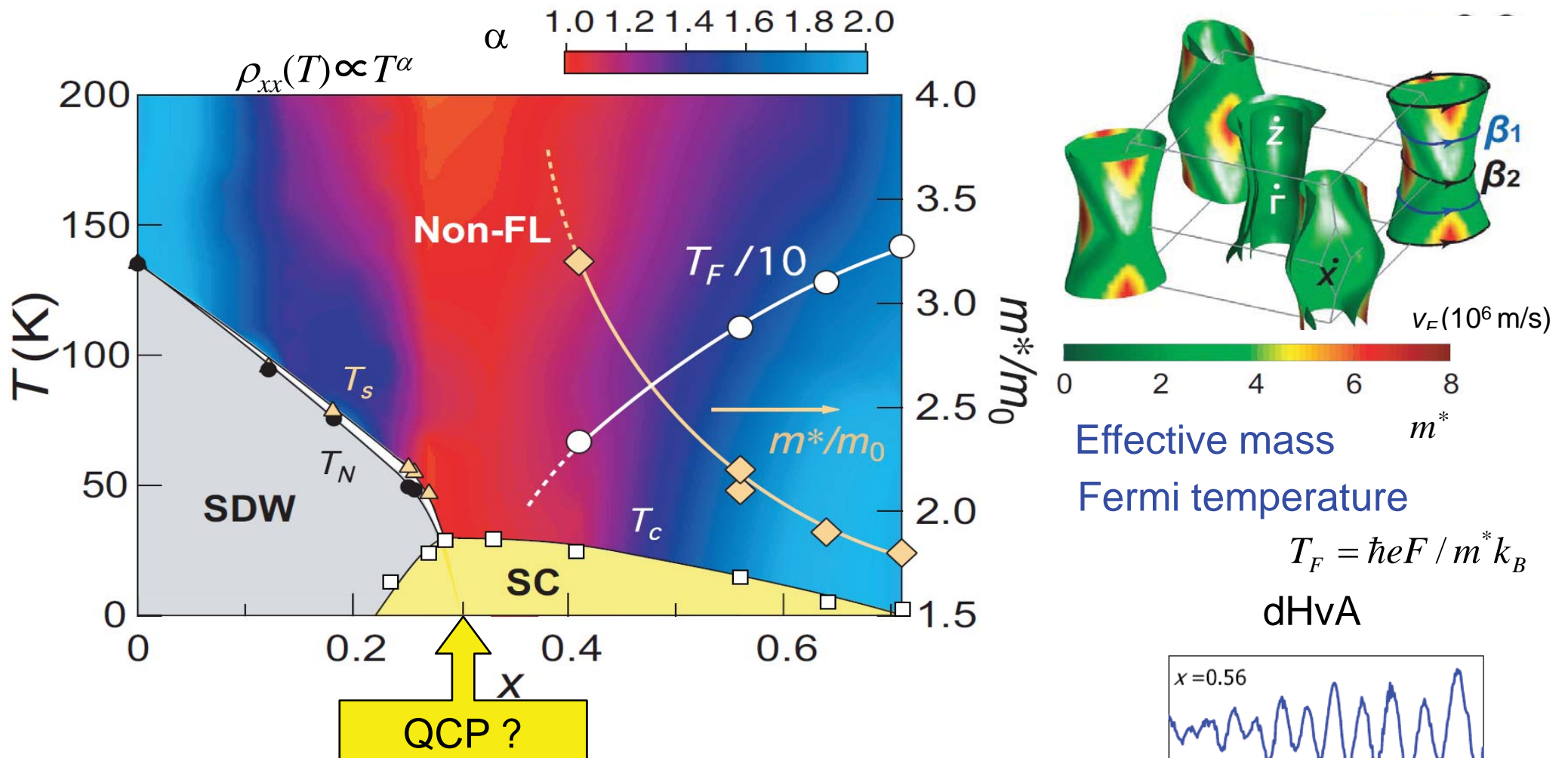
$$T_F = \hbar e F / m^* k_B$$

dHvA



H.Shishido et al. PRL (2009).

Doping evolution of electronic properties above T_c

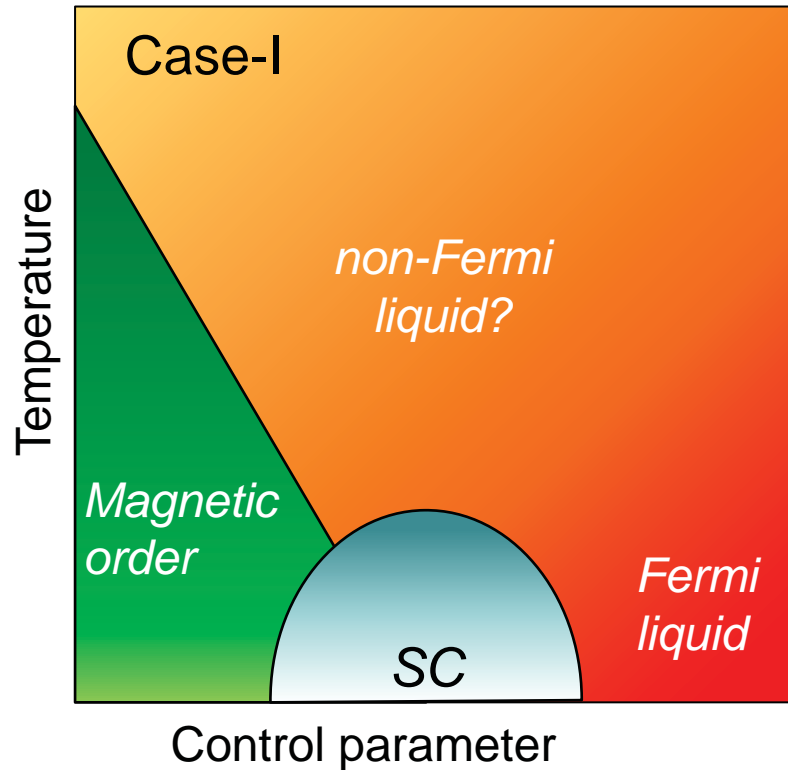


How does the QCP affects the SC properties below T_c ?
 Effective mass m^* is strongly enhanced

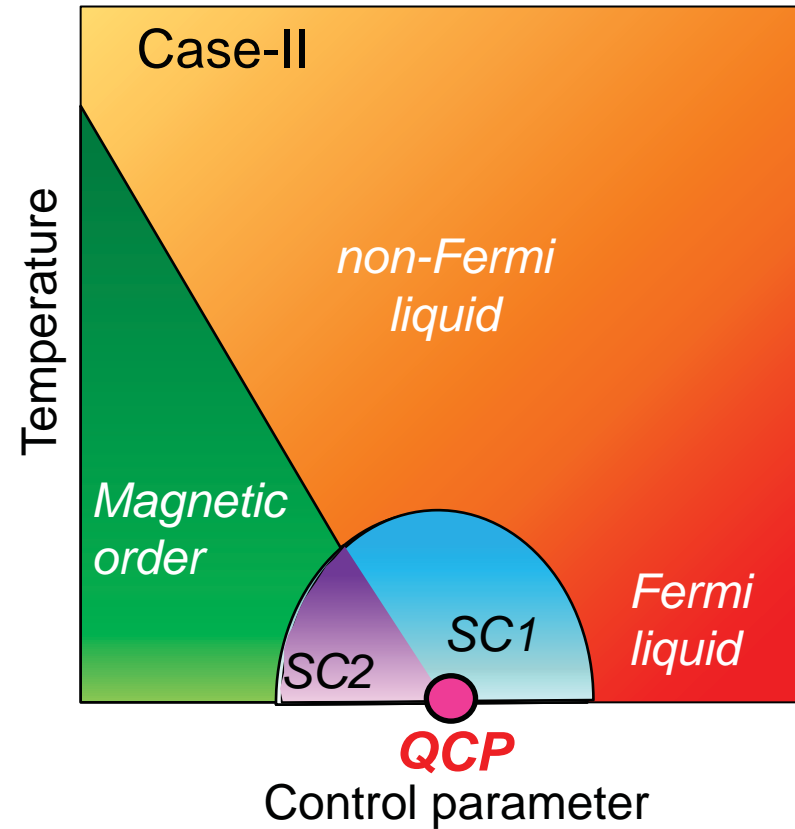
Fermi temperature $T_F = \hbar e F / m^* k_B$ tends to zero

$\mu_0 H(T)$
 H.Shishido et al. PRL (2009).

Does a QCP lie beneath the SC dome?



Criticality avoided by the transition to the SC state



QCP lying beneath the SC dome

A quantum phase transition inside the dome

Two different SC phases.

Superfluid density as a probe of QCP inside the SC dome

London penetration depth λ_L is the quantity that can probe the electronic structure **at the zero-temperature limit.**

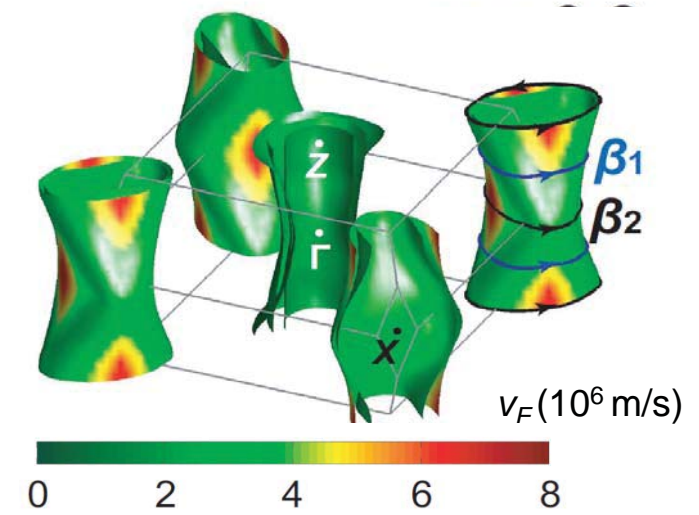
$$\lambda_L^2(0) = \frac{m^*}{\mu_0 n_s e^2}$$

mass of superconducting electrons
density of superconducting electrons

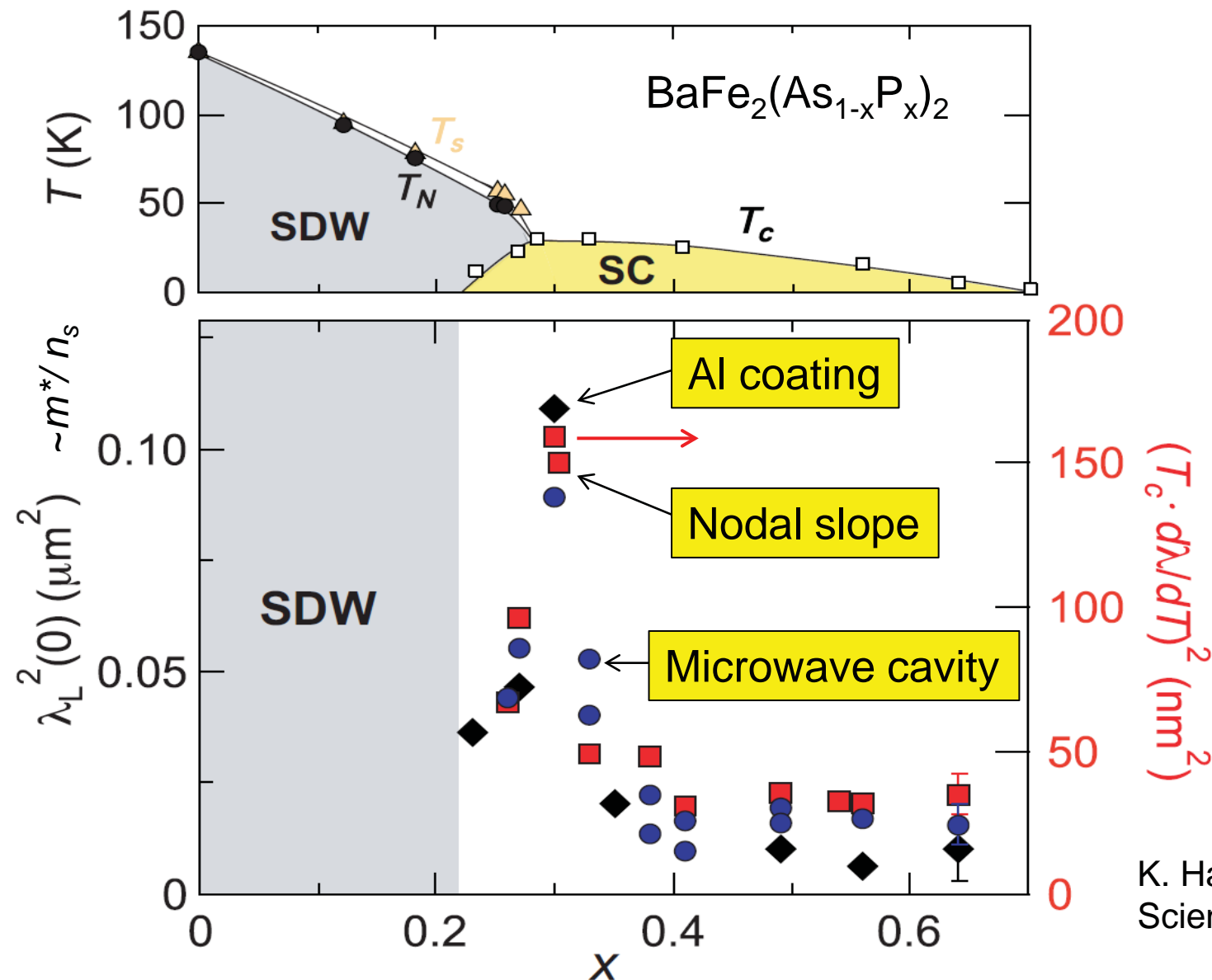
1. Tunnel diode oscillator (13MHz, 70 mK)
Al coated method
2. Microwave surface impedance
Rutile cavity resonator (5 GHz, $Q \sim 10^6$)
3. Nodal superconducting gap structure

Slope of the T -dependence

$$\frac{\delta \lambda_L(T)}{\lambda_L(0)} \approx \frac{\ln 2}{\Delta} k_B T$$



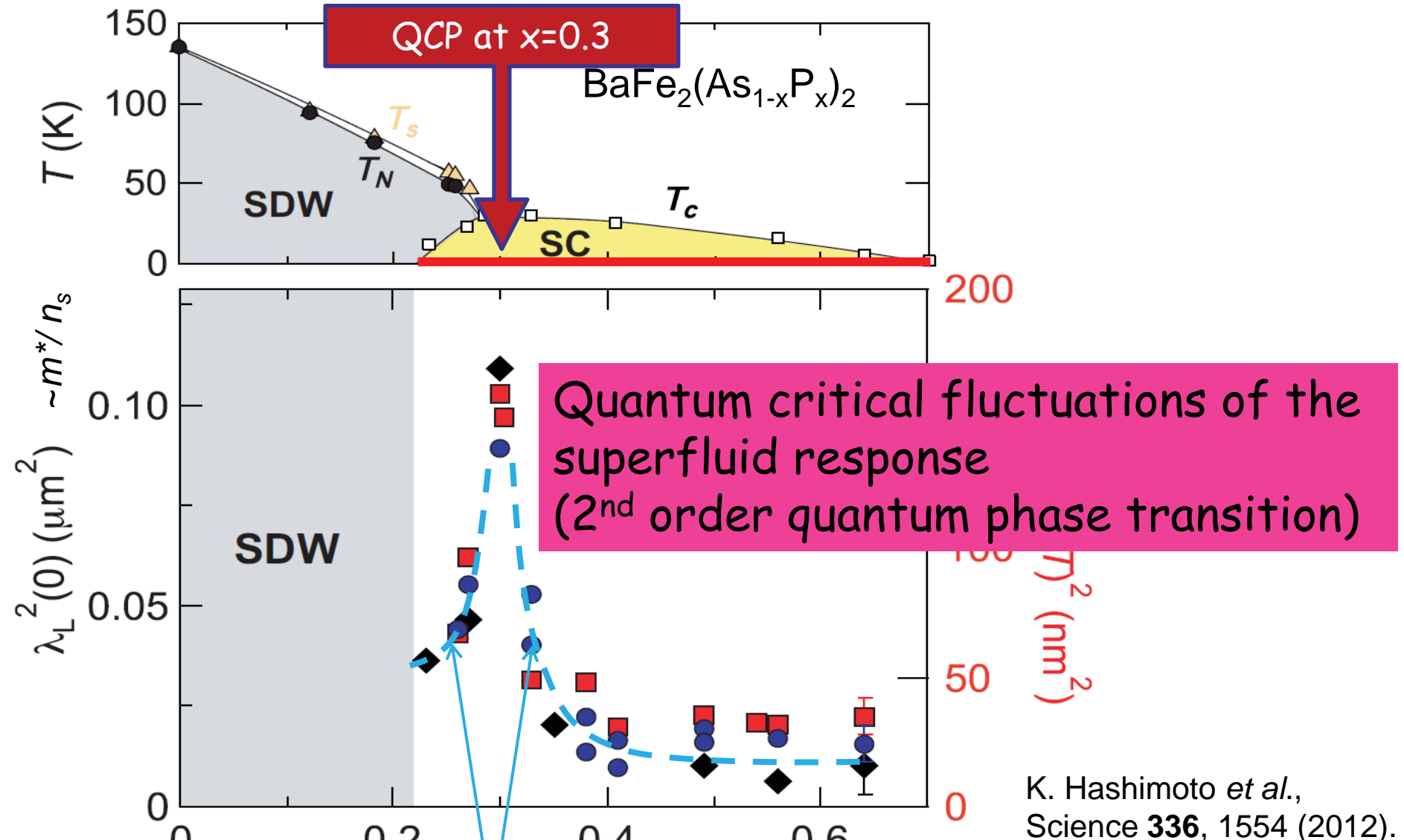
Doping evolution of the London penetration depth at $T=0$



K. Hashimoto *et al.*,
Science 336, 1554 (2012).

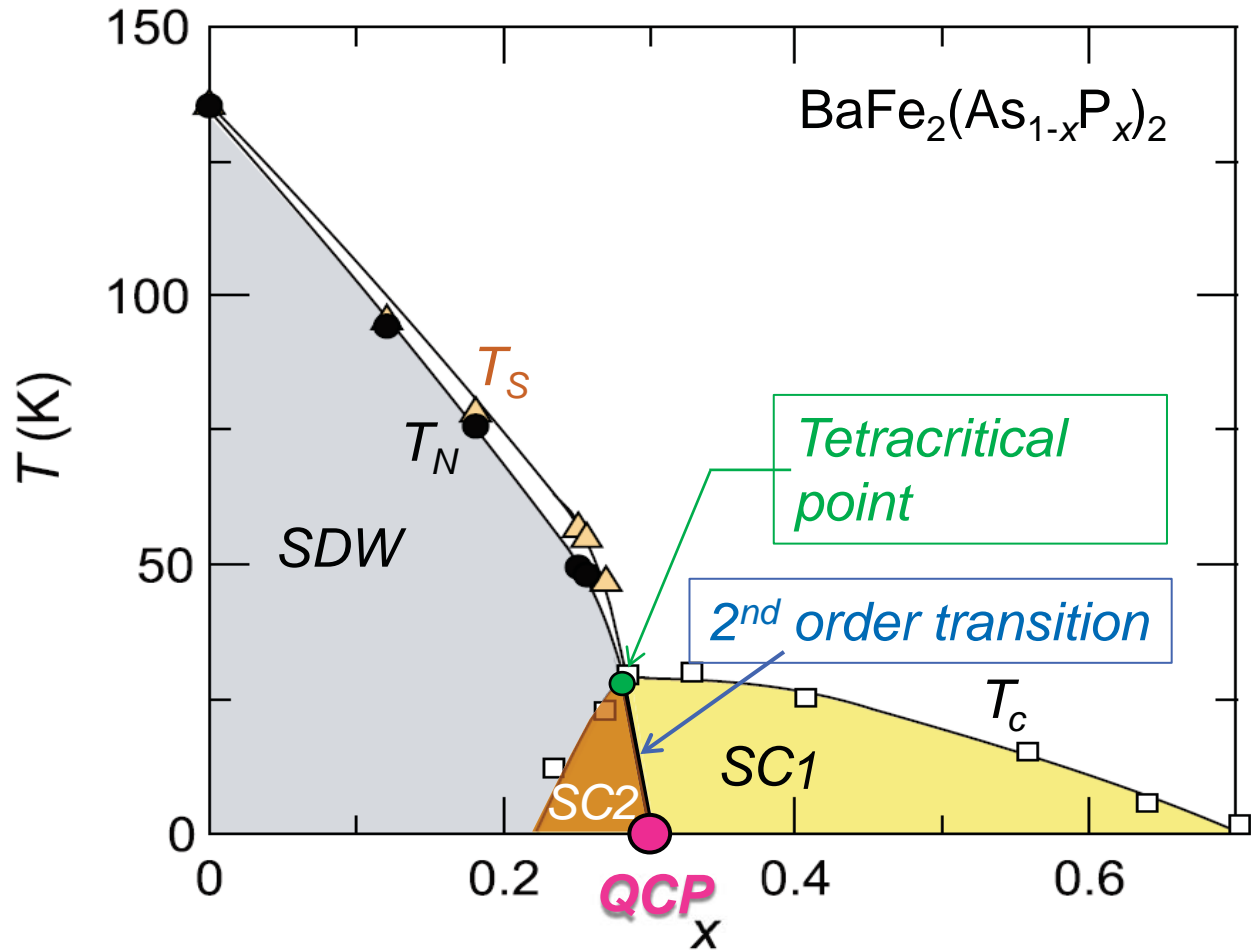
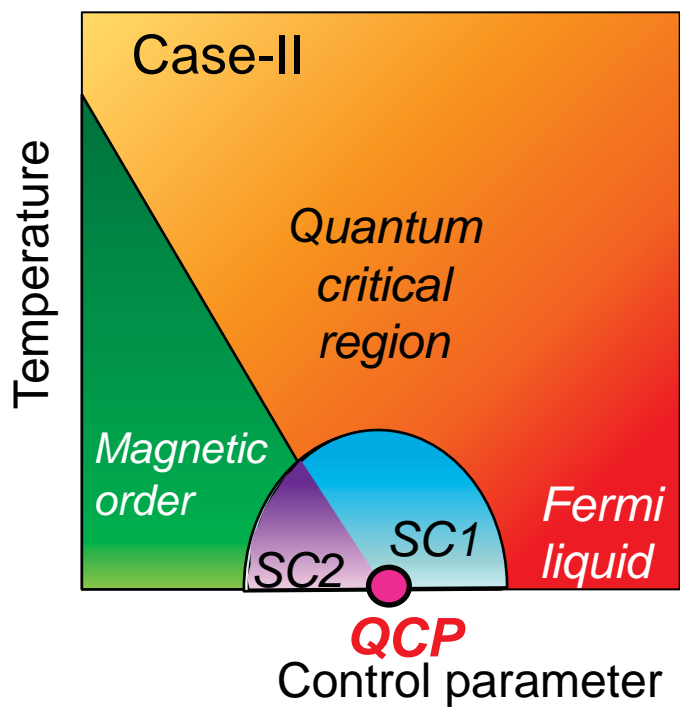
All three methods give very similar x -dependence of $\lambda(0)$.

Doping evolution of the London penetration depth at $T=0$



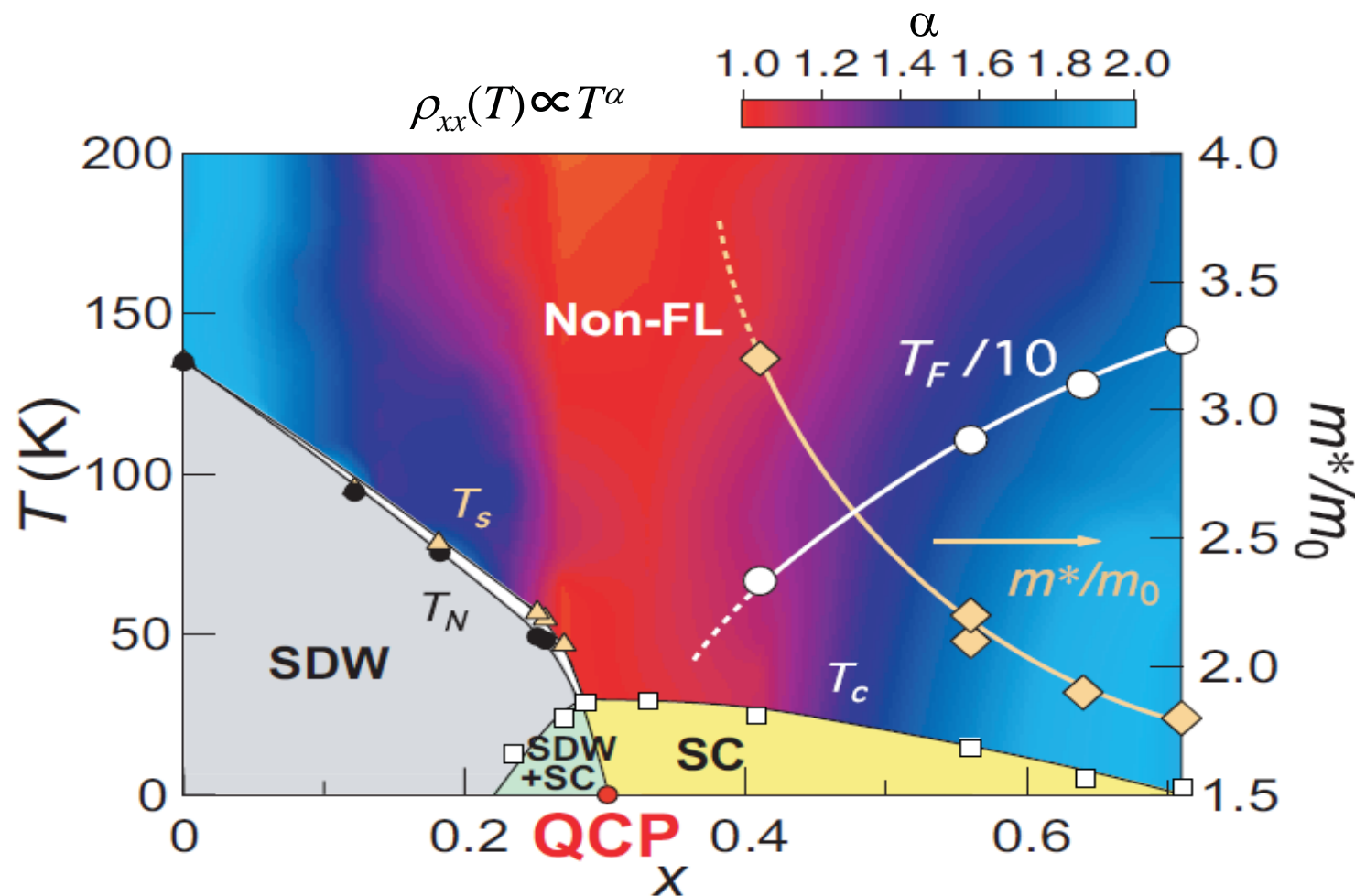
Striking enhancement of $\lambda_L^2(0)$ on approaching $x=0.3$ from *either* side.
The data represents the behavior at the zero temperature limit.

QCP at $x=0.3$



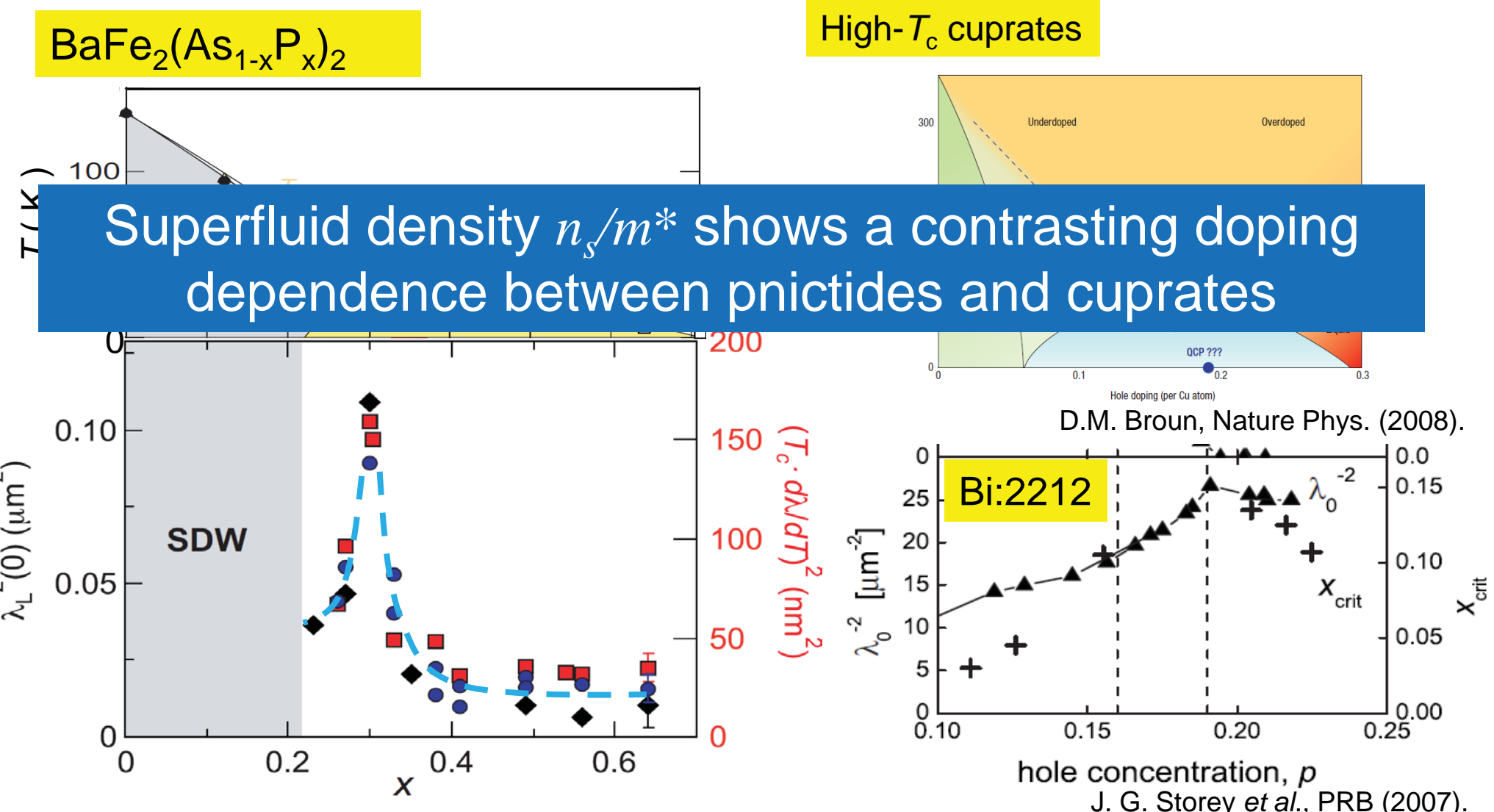
Two distinct SC phases

QCP at $x=0.3$



The mass enhancement, reduction of Fermi temperature and non-Fermi liquid behavior, all are associated with the finite-temperature quantum critical region linked to the QCP.

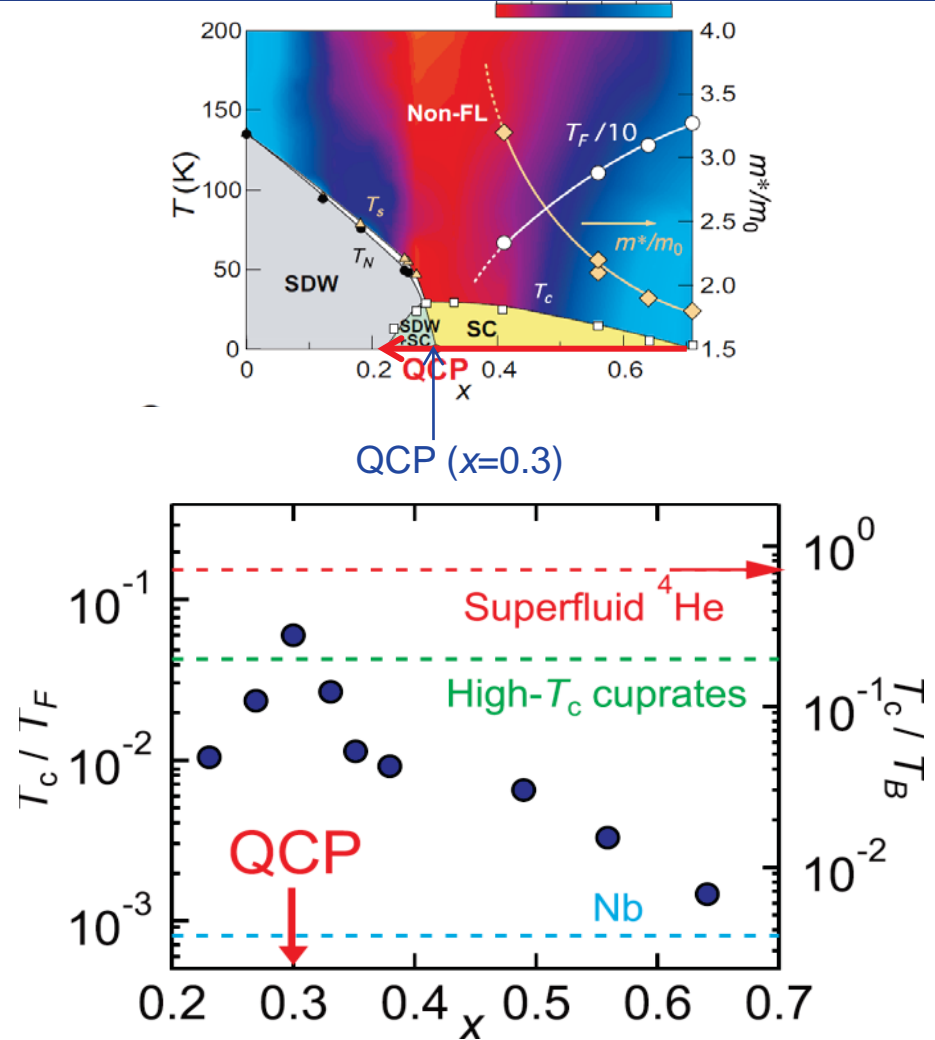
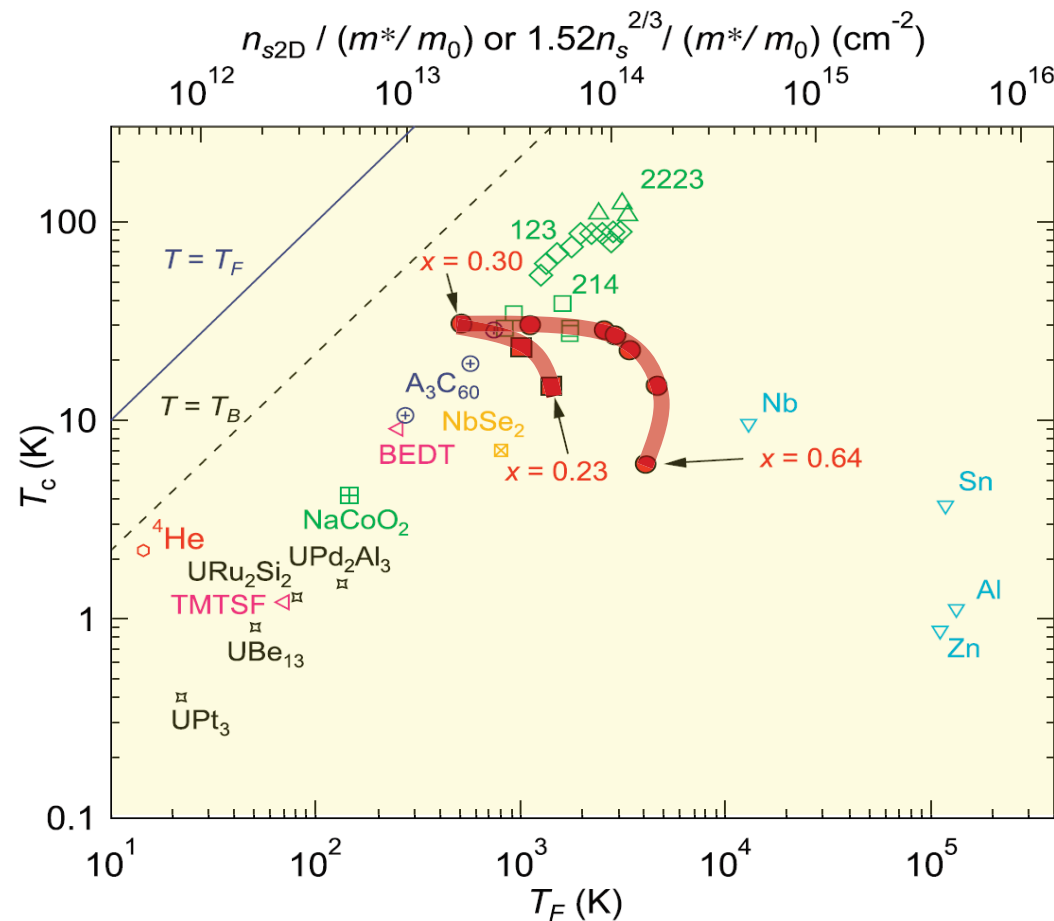
Doping evolution of the London penetration depth at $T=0$



Bi:2212 : broad maximum in $1/\lambda_L^2(0)$ (enhancement of n_s/m^*) at $p \sim 0.19$

BaFe₂(As_{1-x}P_x)₂ : sharp peak in $\lambda_L^2(0)$ (suppression of n_s/m^*) at $x=0.3$

Doping evolution of the superfluid density (Uemura plot)

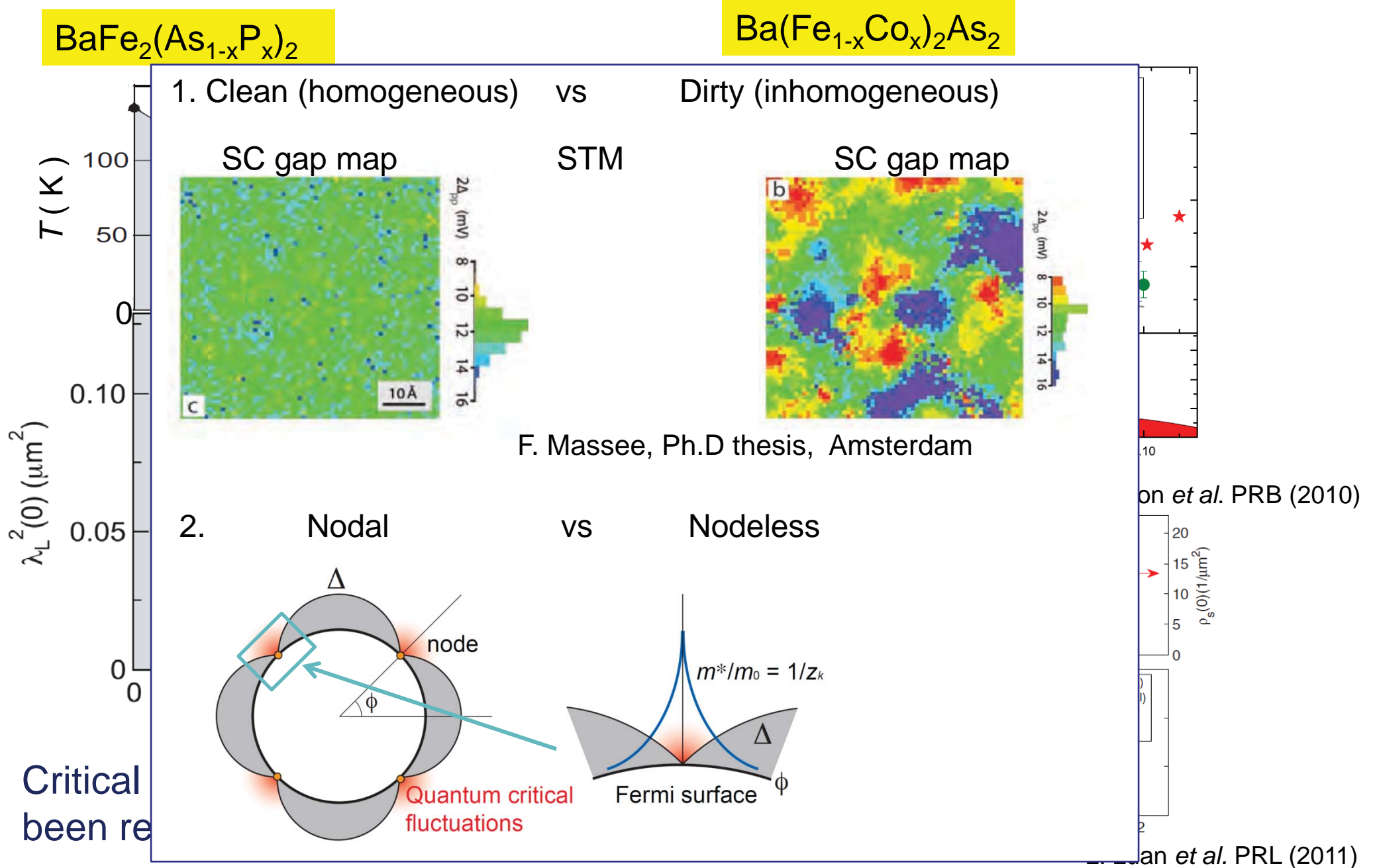


The strongest pairing interaction at the QCP.



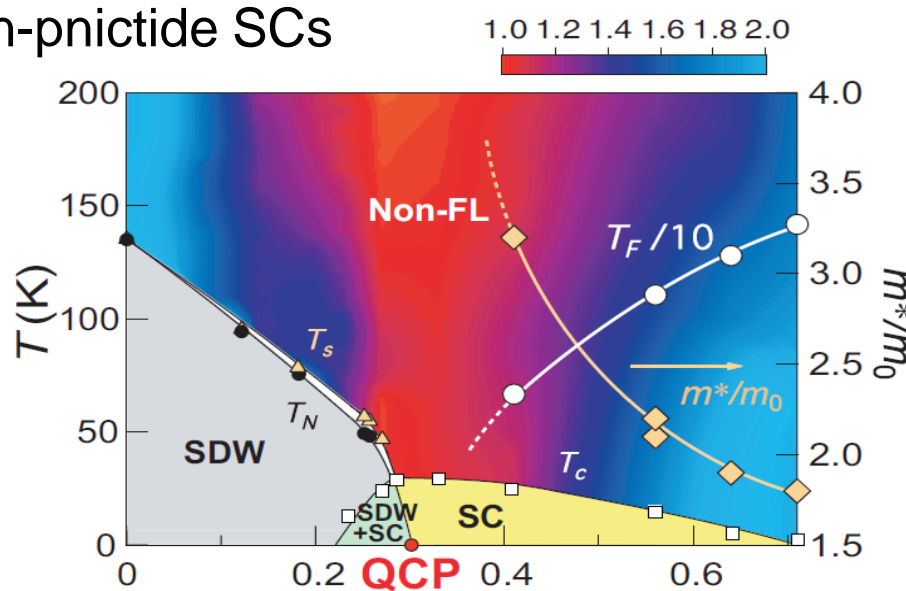
High- T_c SC may be driven by the QCP

Comparison with P-doped and Co-doped systems

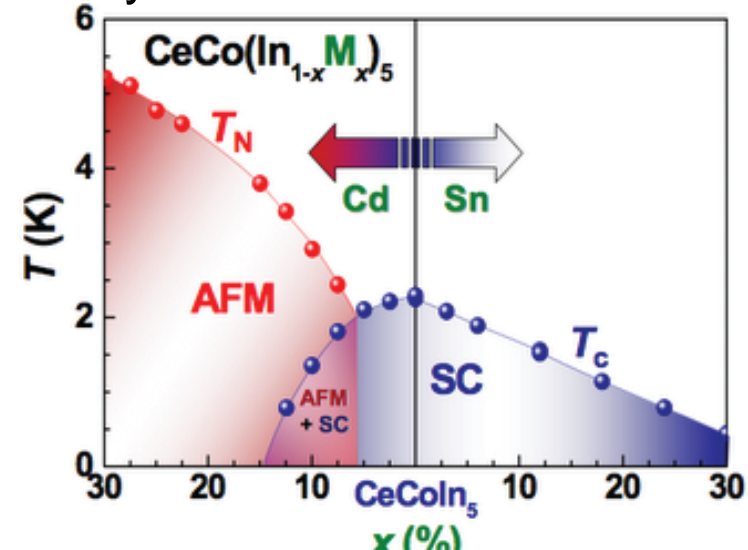


Nodal superconductors in the vicinity of AFM

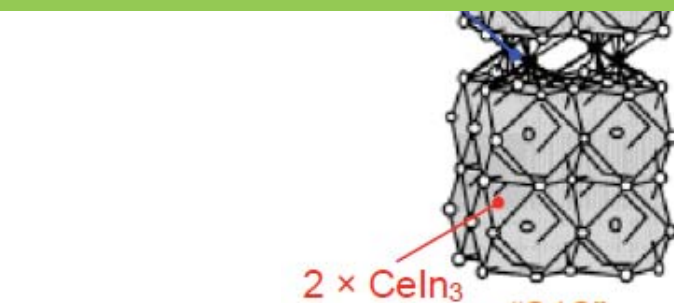
Iron-pnictide SCs



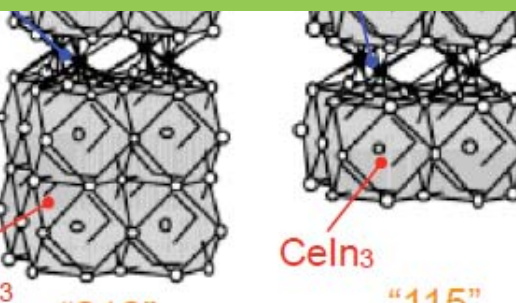
Heavy-Fermion SCs



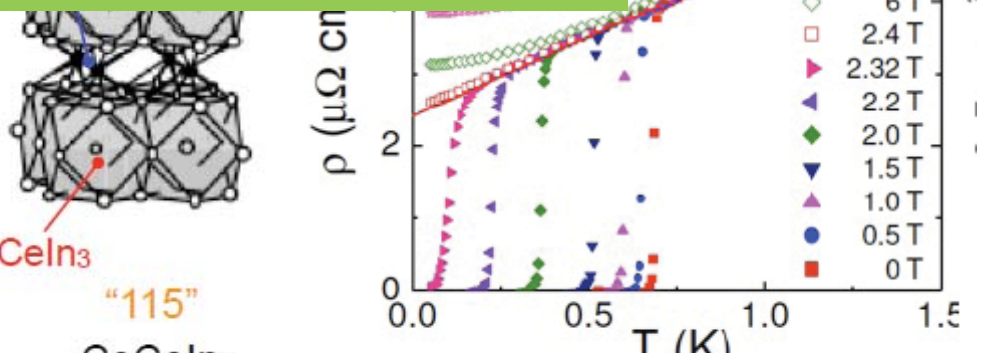
The effect of quantum fluctuations on the low-energy quasiparticle excitations from the SC ground state is not well established.



D. Kaczorowski *et al.*,
PRL (2009).

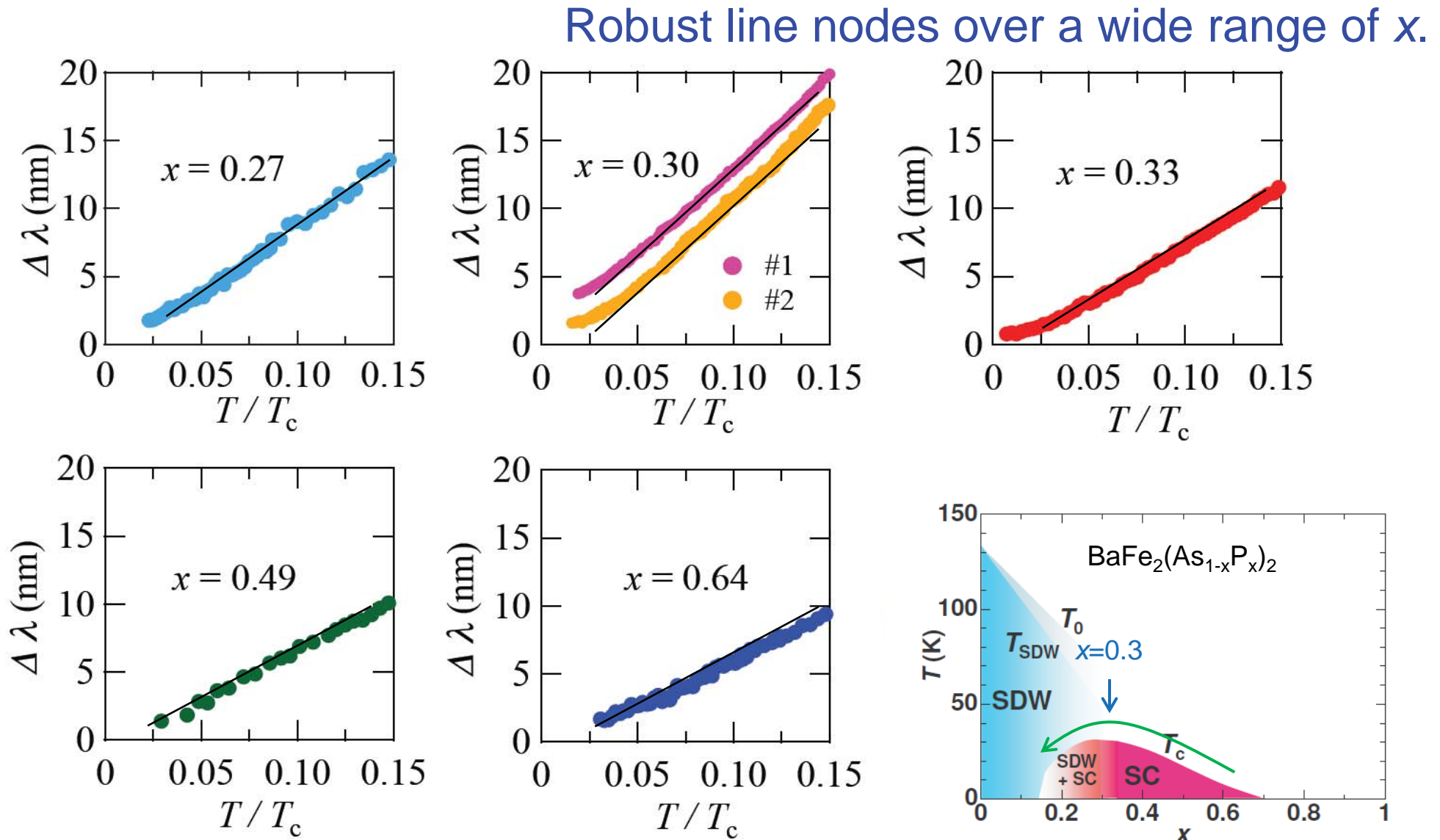


$T_c = 0.68$ K



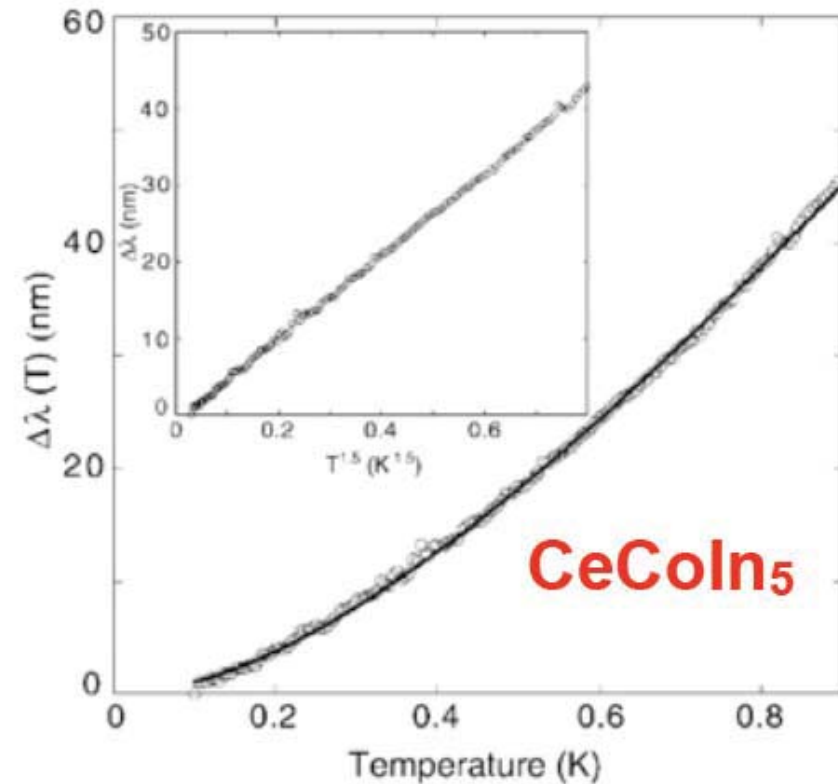
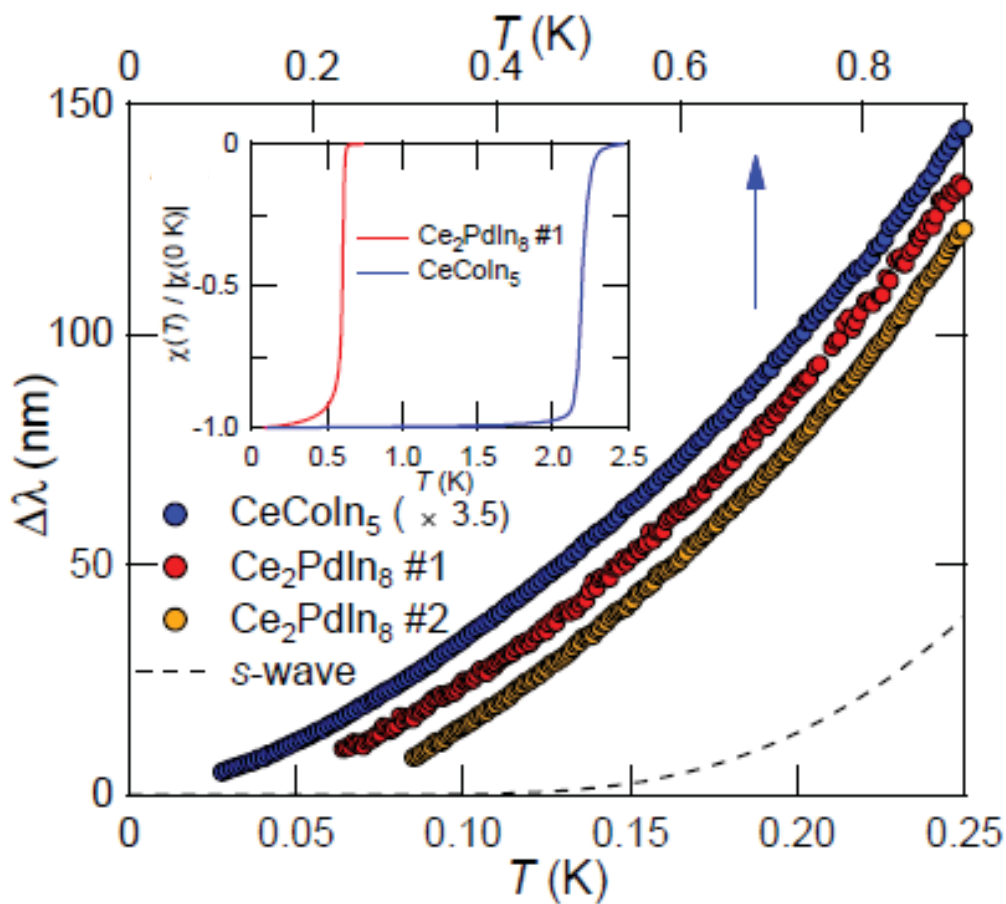
J. K. Dong *et al.*, PRX 1, 011010 (2011).

Doping evolution of $\lambda(T)$ in $\text{BaFe}_2(\text{As},\text{P})_2$



Deviations from the T -linear dependence near $x=0.3$

Anomalous $\lambda(T)$ in CeColn₅ and Ce₂PdIn₈

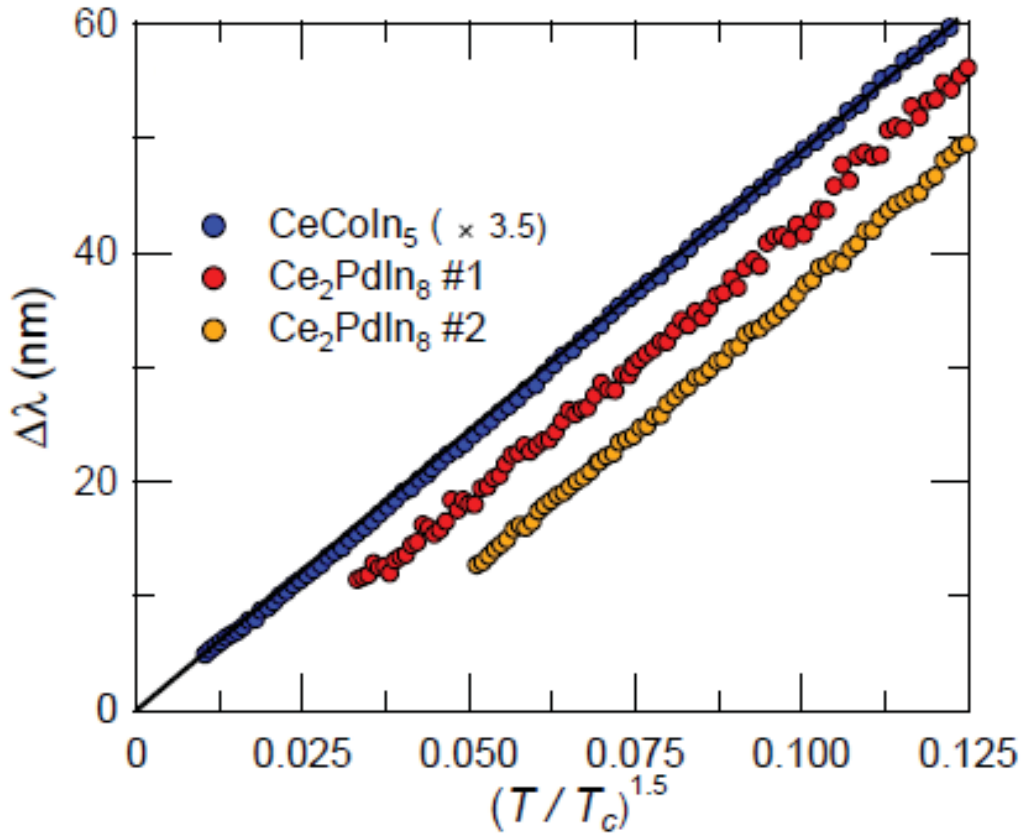
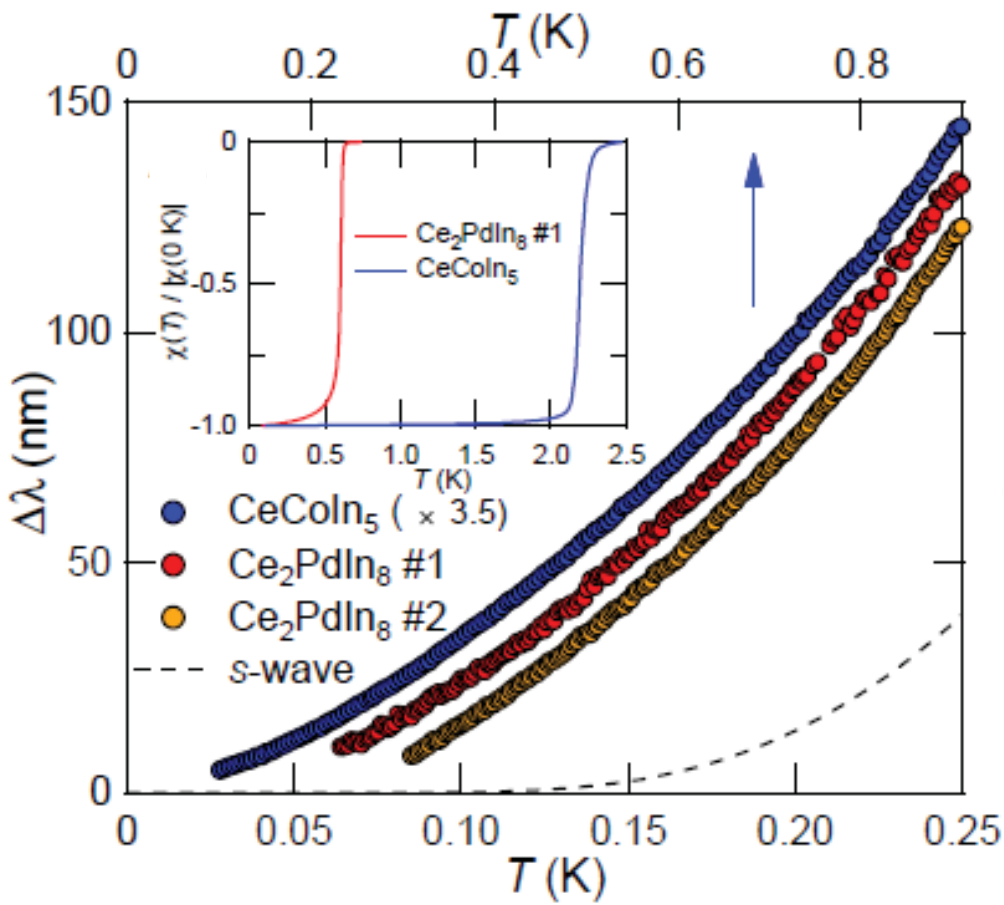


Deviations from the T -linear dependence

Consistent with previous studies.

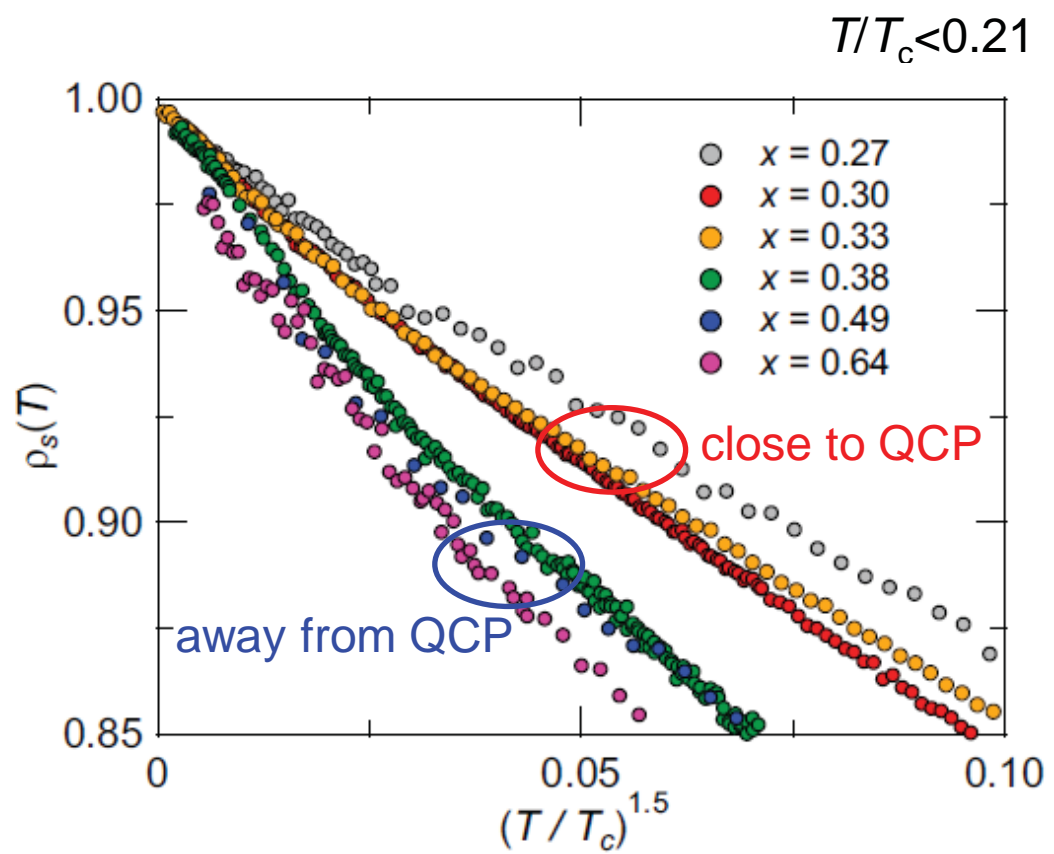
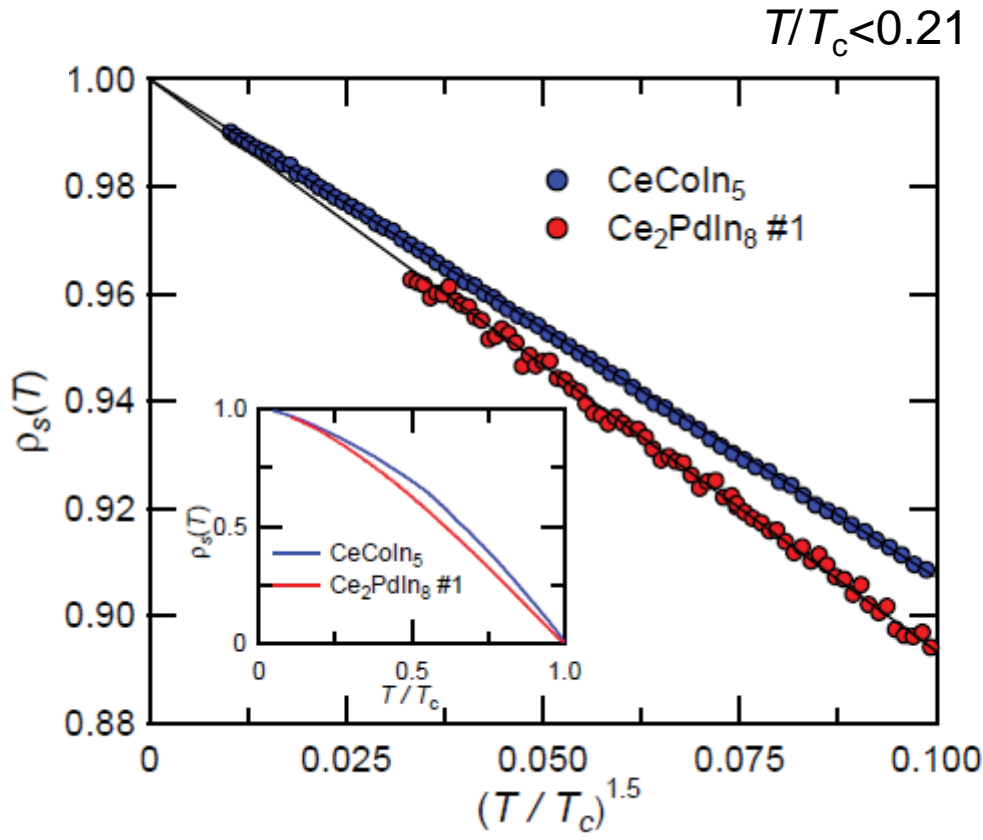
S. Ozcan *et al.*, Europhys. Lett **62** 412 (2003).

Anomalous $\lambda(T)$ in CeCoIn₅ and Ce₂PdIn₈

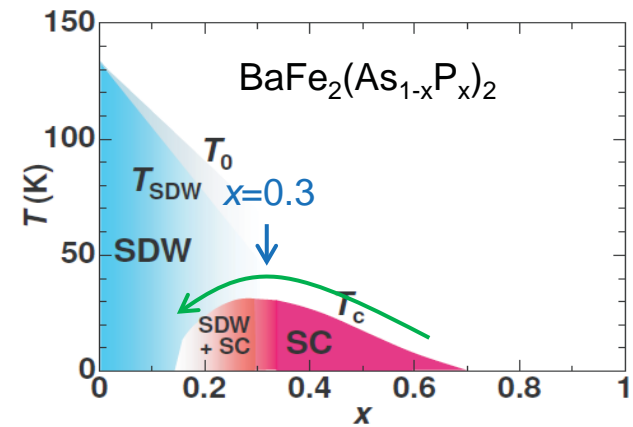


Anomalous non-integer 3/2 power-law dependence in a wide T -range

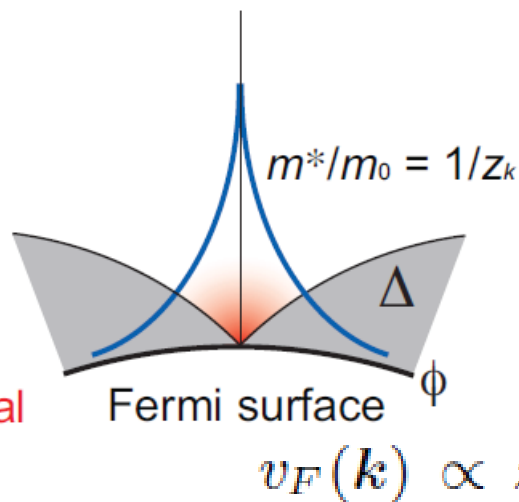
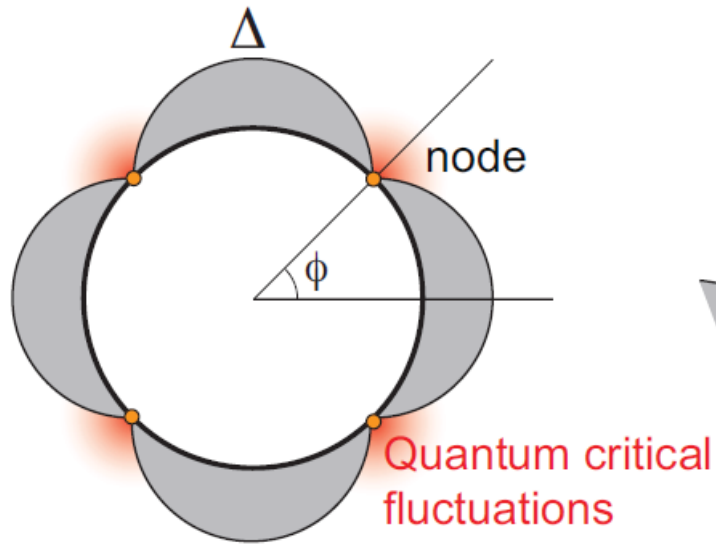
Anomalous superfluid density in ‘quantum critical’ SCs



Anomalous non-integer power-law T dependence of superfluid density (except for the very low- T) is observed.



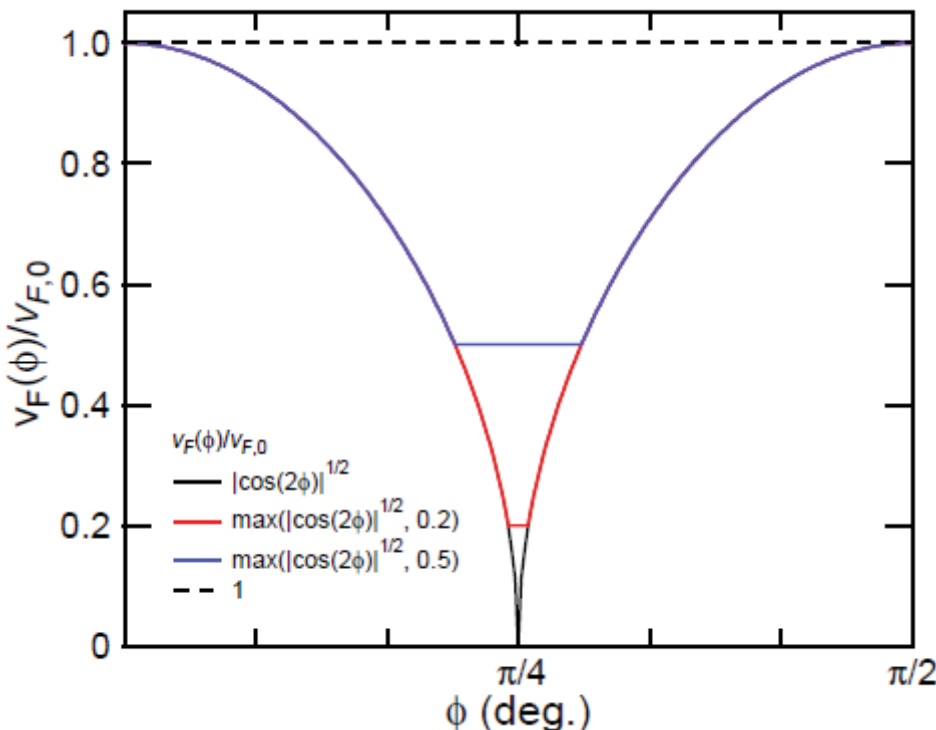
'Nodal quantum criticality' in unconventional SCs



$m^{*2} \propto (p - p_{QCP})^{-\beta}$
 p : non-thermal parameter
 $\beta \sim 1$ has been reported
in $\beta\text{-YbAlB}_4$ and YbRh_2Si_2

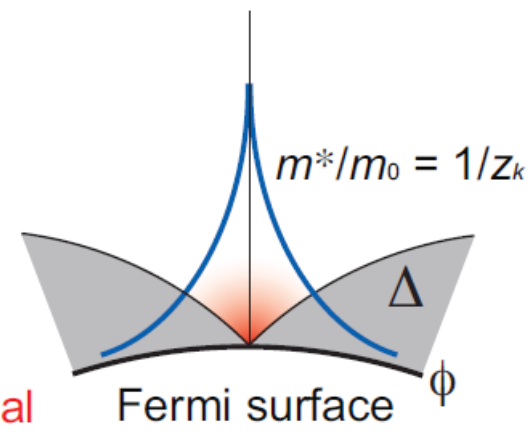
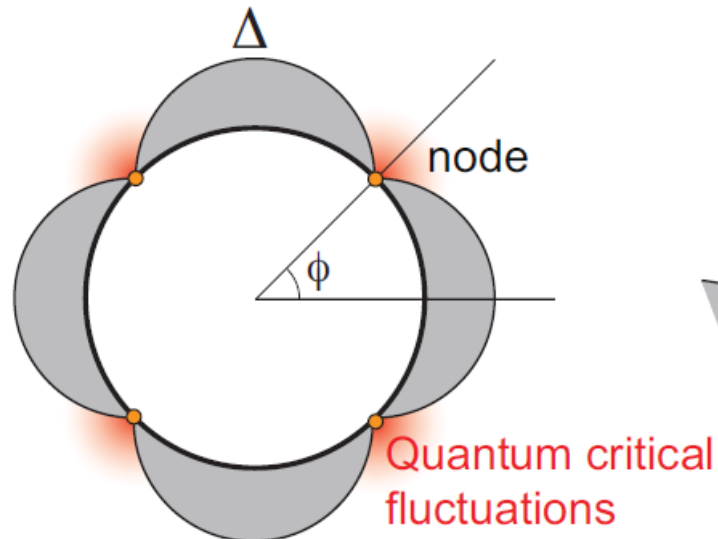
Y. Matsumoto *et al.*, Science (2011).
P. Gegenwart *et al.*, PRL (2002).

$$v_F(k) \propto z_k \propto 1/m^*(k) \propto |\Delta(k)|^{\beta/2}$$



Low-energy quantum critical fluctuations
may be quenched by the SC gap formation.
↓
Degree of quenching low-energy fluctuations
may be determined by the gap magnitude.

'Nodal quantum criticality' in unconventional SCs



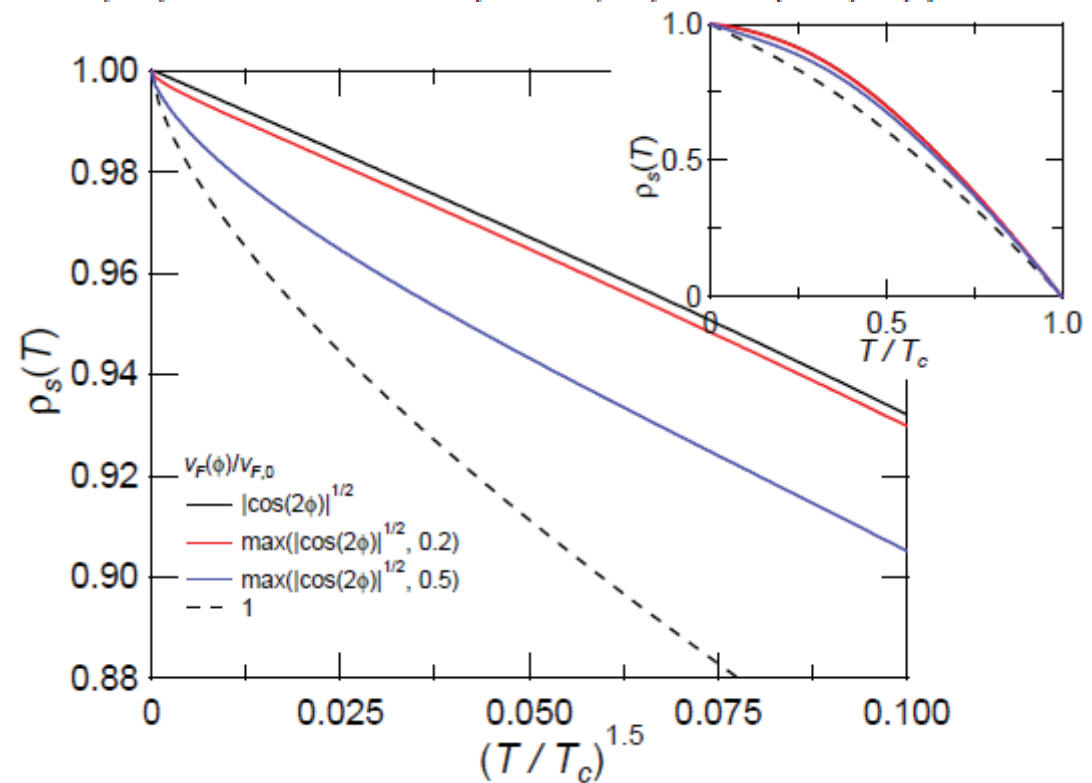
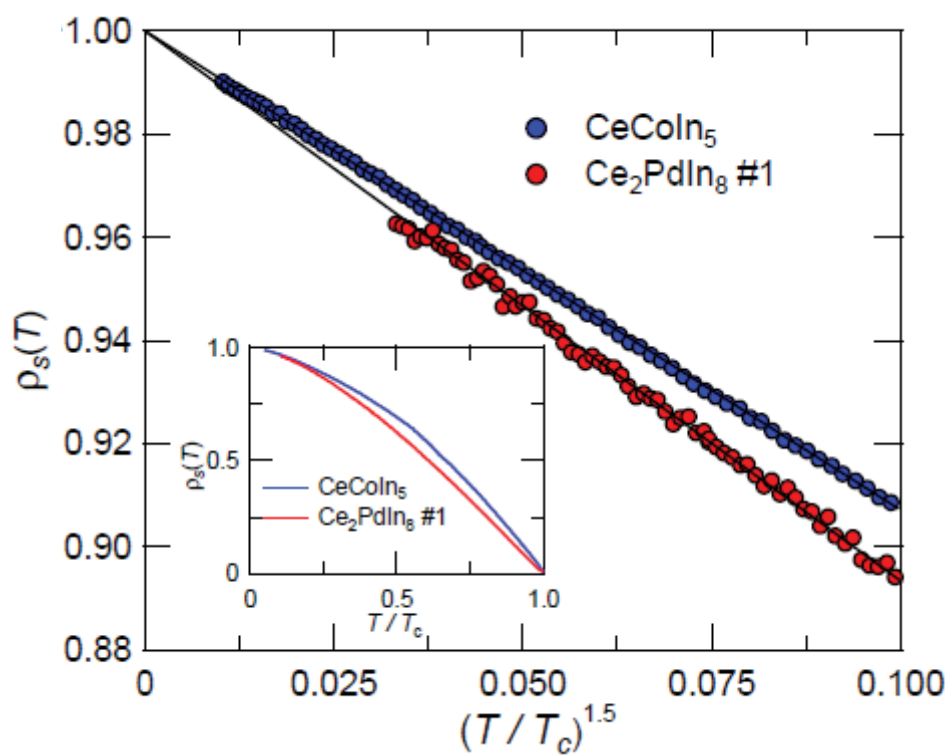
$$m^{*2} \propto (p - p_{QCP})^{-\beta}$$

p : non-thermal parameter

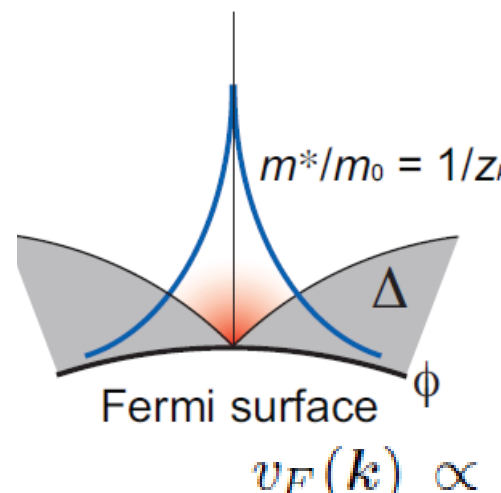
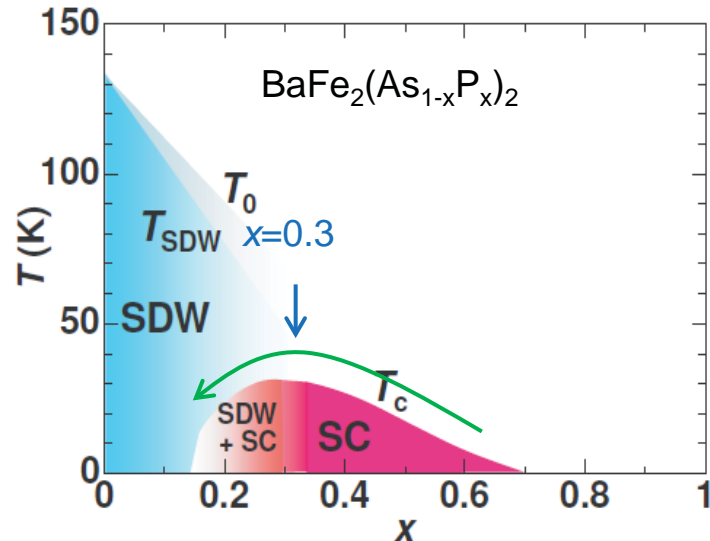
$\beta \sim 1$ has been reported
in $\beta\text{-YbAlB}_4$ and YbRh_2Si_2

Y. Matsumoto *et al.*, Science (2011).
P. Gegenwart *et al.*, PRL (2002).

$$v_F(k) \propto z_k \propto 1/m^*(k) \propto |\Delta(k)|^{\beta/2}$$



'Nodal quantum criticality' in unconventional SCs



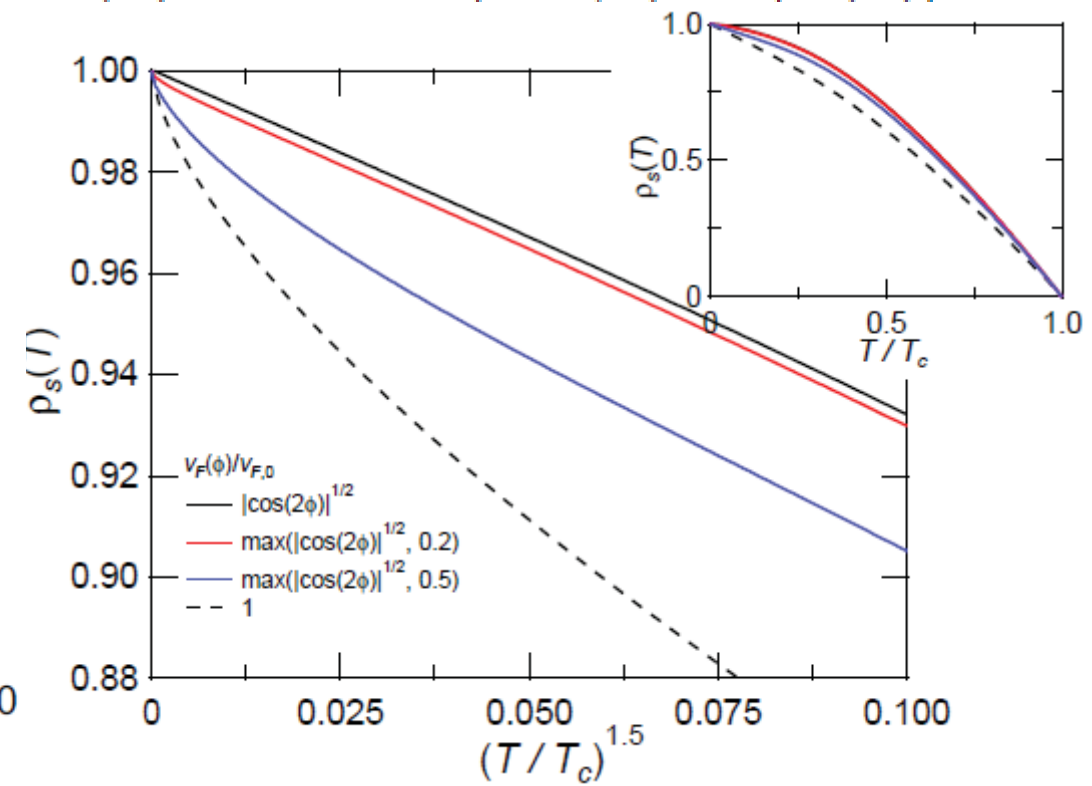
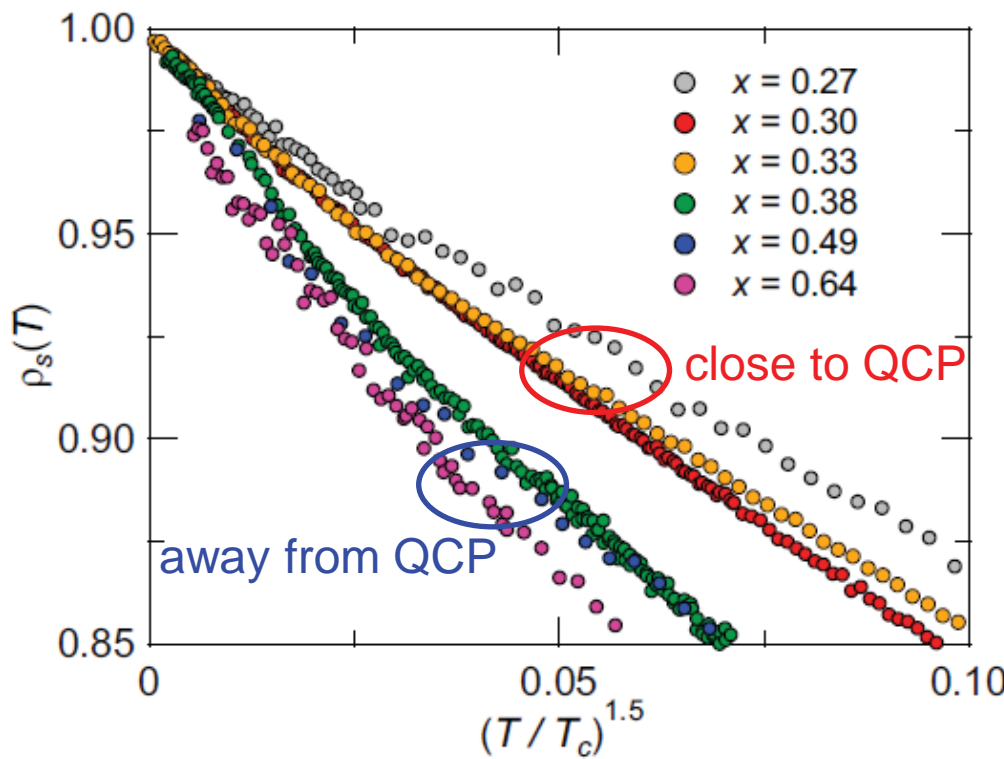
$m^{*2} \propto (p - p_{QCP})^{-\beta}$

p : non-thermal parameter

$\beta \sim 1$ has been reported
in β -YbAlB₄ and YbRh₂Si₂

Y. Matsumoto *et al.*, Science (2011).
P. Gegenwart *et al.*, PRL (2002).

$$v_F(k) \propto z_k \propto 1/m^*(k) \propto |\Delta(k)|^{\beta/2}$$



Nematic transition and antiferromagnetic quantum critical point in $\text{BaFe}_2(\text{As}_{1-x}\text{P}_x)_2$

Taka Shibauchi

Department of Physics, Kyoto University

1. Quantum phase transition lurking inside the superconducting dome

K. Hashimoto *et al.*, Science 336, 1554 (2012).

2. Nematic transition above the dome

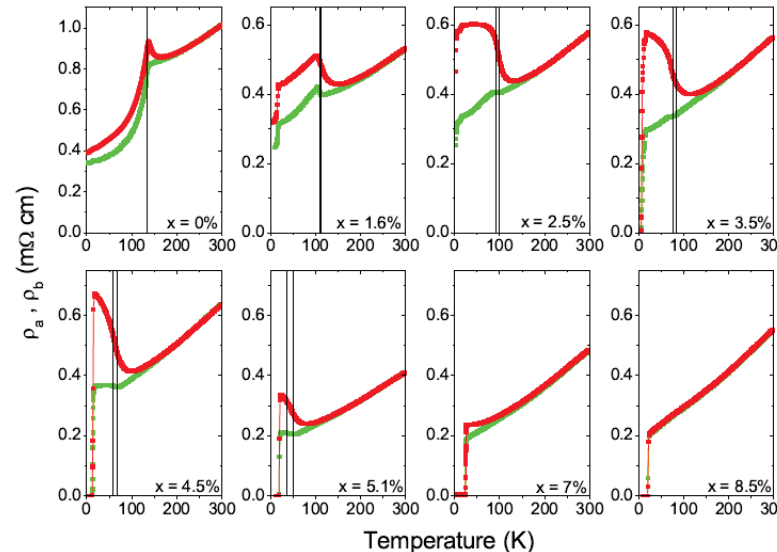
S. Kasahara *et al.*, Nature 486, 382 (2012).

3. Summary – A renewed phase diagram

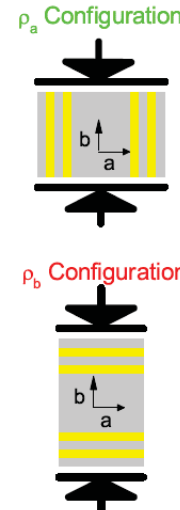


Experiments suggesting in-plane anisotropy at $T > T_s$

★ Resistivity J. Chu *et al.* Science (2010).



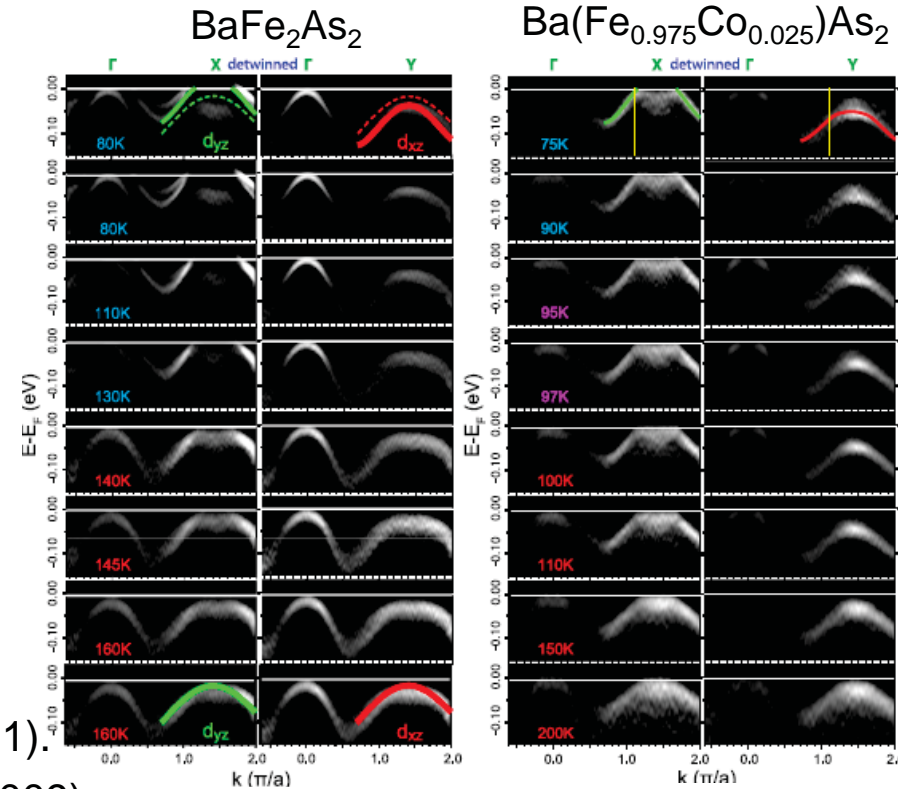
$\rho_b > \rho_a$ above T_s



Detwinned by uniaxial pressure

★ ARPES

M. Yi *et al.*, PNAS (2011).



★ Optical Conductivity A. Dusza *et al.*, EPL (2011).

M. Nakajima *et al.*, PNAS (2011).

★ Neutron Scattering

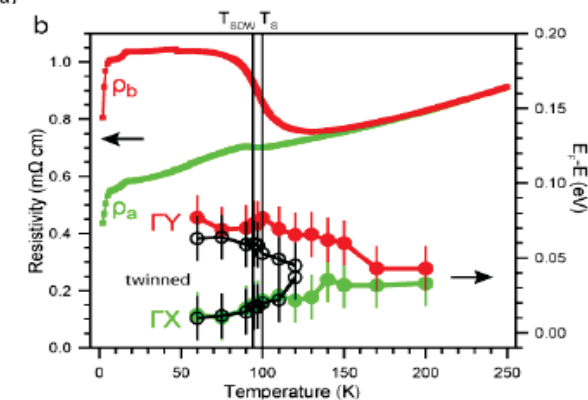
J. Zhao *et al.*, Nature Phys. (2009).

L. W. Harriger *et al.*, PRB (2011).

★ X-Ray Diffraction

E.C. Blomberg *et al.*, PRB (2012).

In-plane anisotropy seems to extend above T_s in crystals under uniaxial strain.



Experiments suggesting in-plane anisotropy at $T > T_s$

Uniaxial pressure itself breaks the rotational symmetry and may induce the in-plane anisotropy.

To address whether unidirectional self-organization of electrons (nematicity) occurs above T_s or not, we need experiments *without* uniaxial pressure.

What the magnetic torque tells us

$$\tau = \mu_0 M V \times H$$

$$M_i = \sum_j \chi_{ij} H_j$$

τ : magnetic torque

V : sample volume

M : magnetization

H : applied Field

Magnetic Torque: Thermodynamic Quantity

★ Micro-cantilever

Very high sensitivity

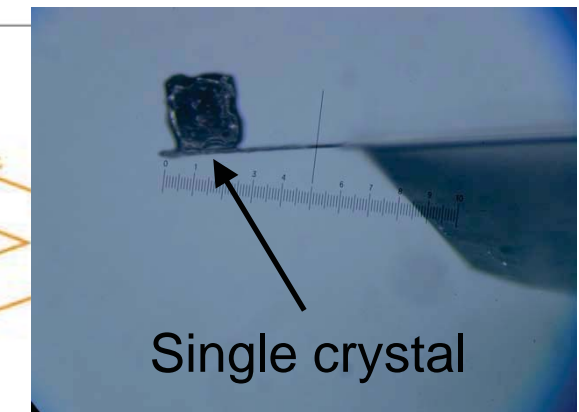
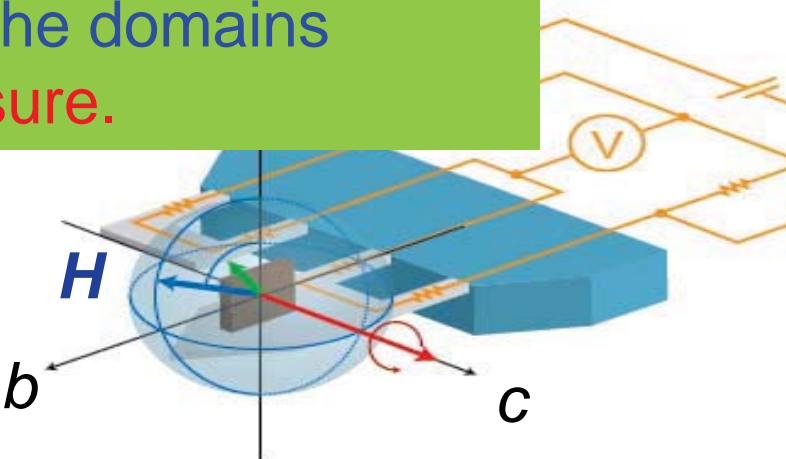
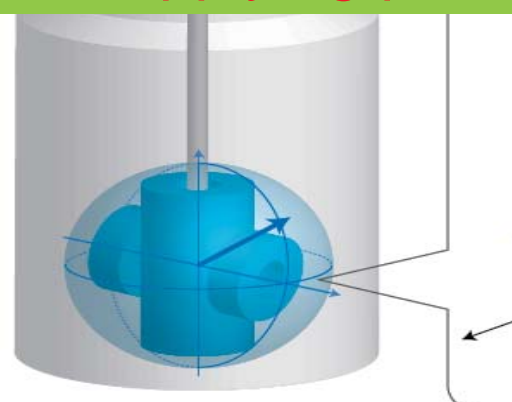
torque 5×10^{-12} e.m.u.
SQUID 10^{-8} e.m.u.] $> 10^3 !!$
(at $\mu_0 H = 4T$)

★ A tiny pure single crystal

(Typical crystal dimensions: $70 \times 70 \times 30 \text{ }\mu\text{m}^3$)

★ Precise control of the field directions within ab plane

In tiny crystals, we have a good chance
to have **imbalance of the domains**
without applying pressure.

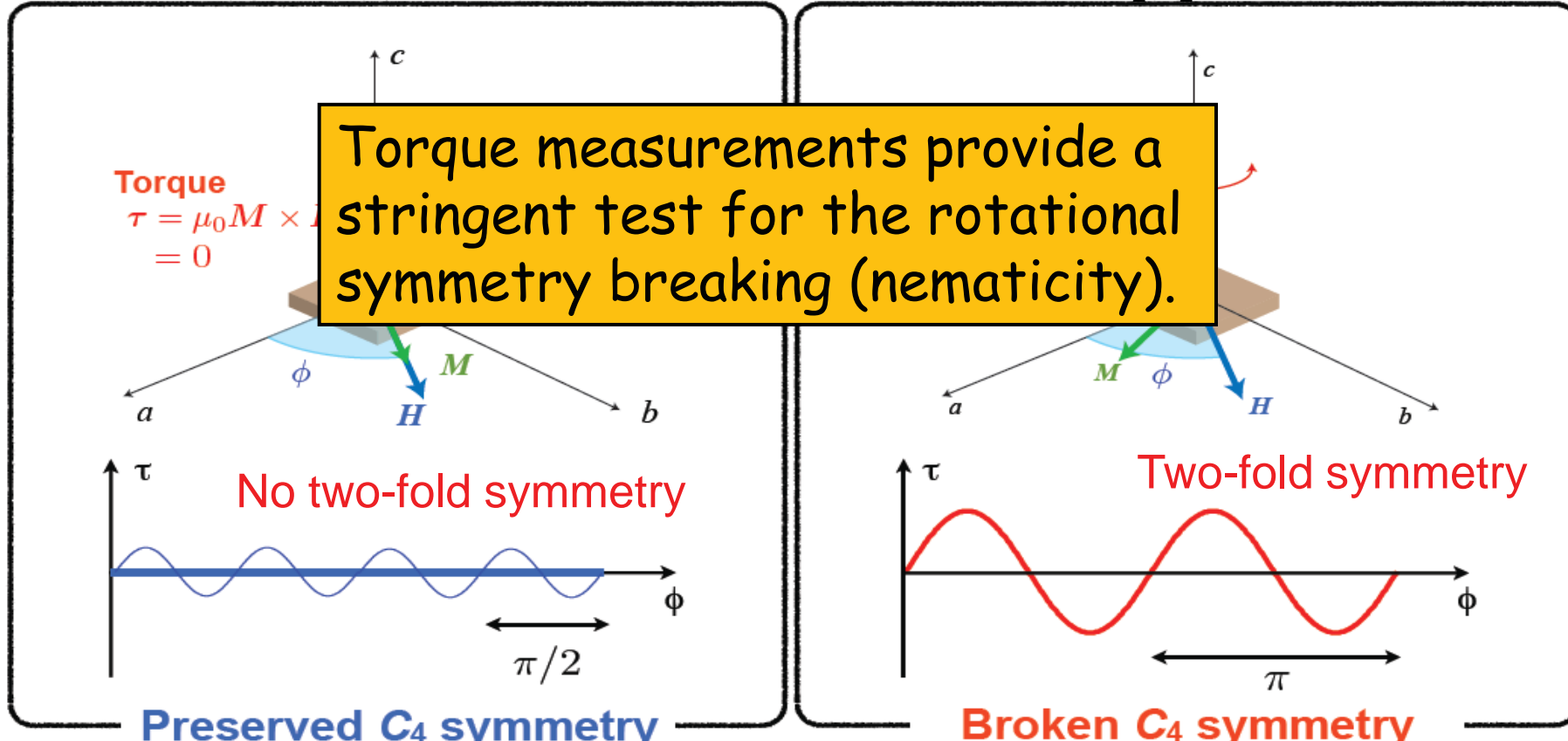


Vector magnet & Mechanical rotator

What the magnetic torque tells us

H rotation within the ab plane

see R. Okazaki, TS et al., Science (2011)
for URu_2Si_2 results.



$$M_i = \sum_j \chi_{ij} H_j$$

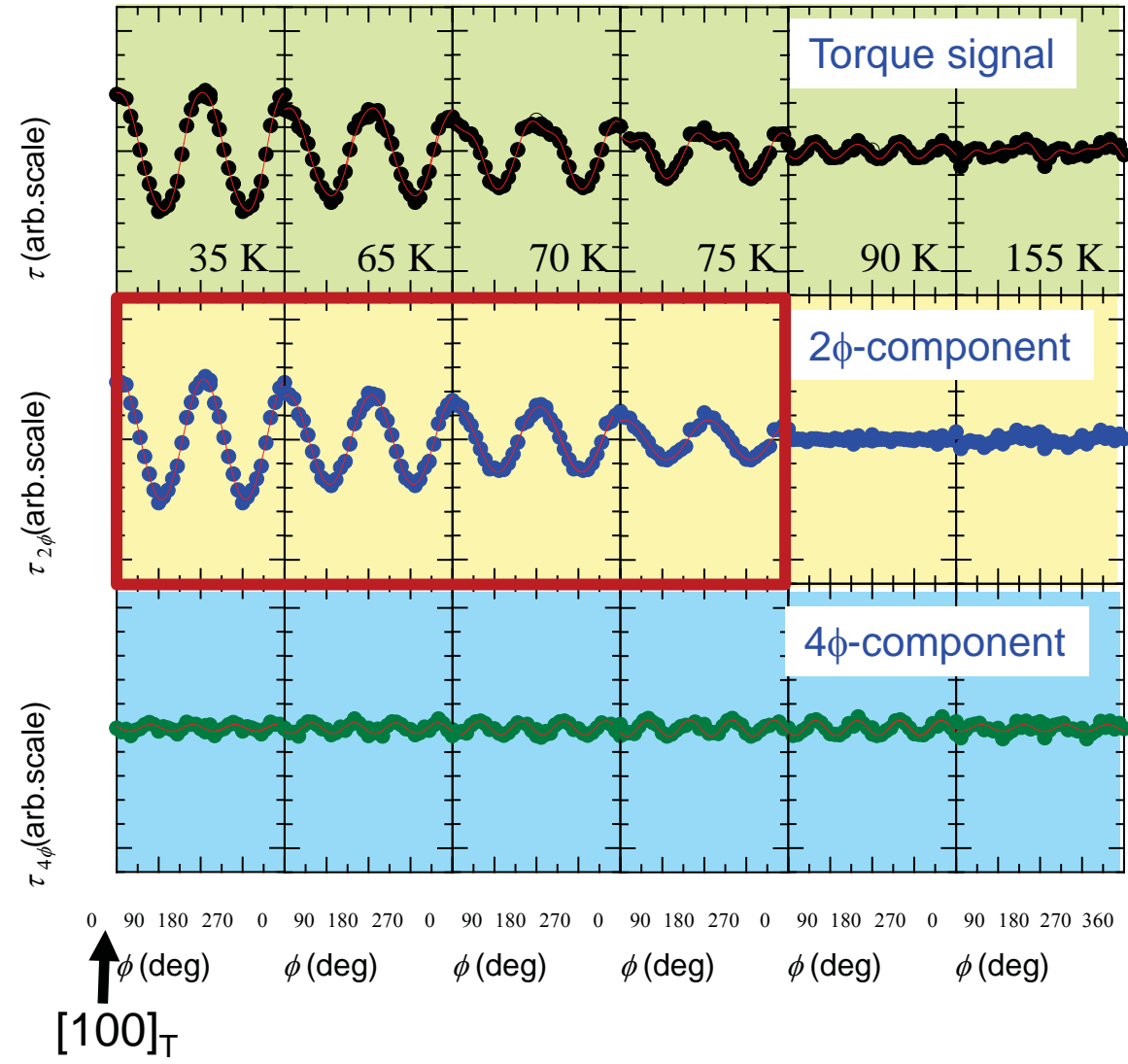
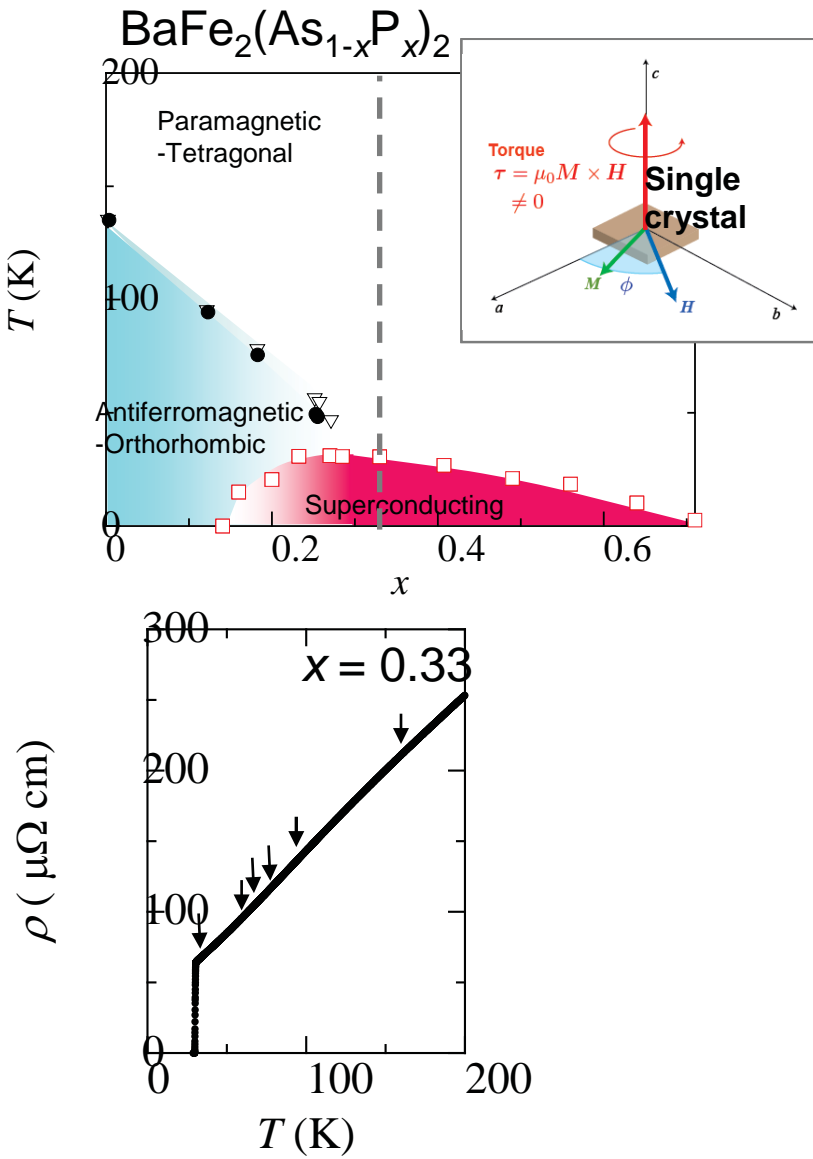
$$\tau = \mu_0 M V \times H$$

$$\tau = \frac{1}{2} \mu_0 H^2 V [(\chi_{aa} - \chi_{bb}) \sin 2\phi - 2\chi_{ab} \cos 2\phi]$$

$\chi_{aa} = \chi_{bb}$ and $\chi_{ab} = 0$

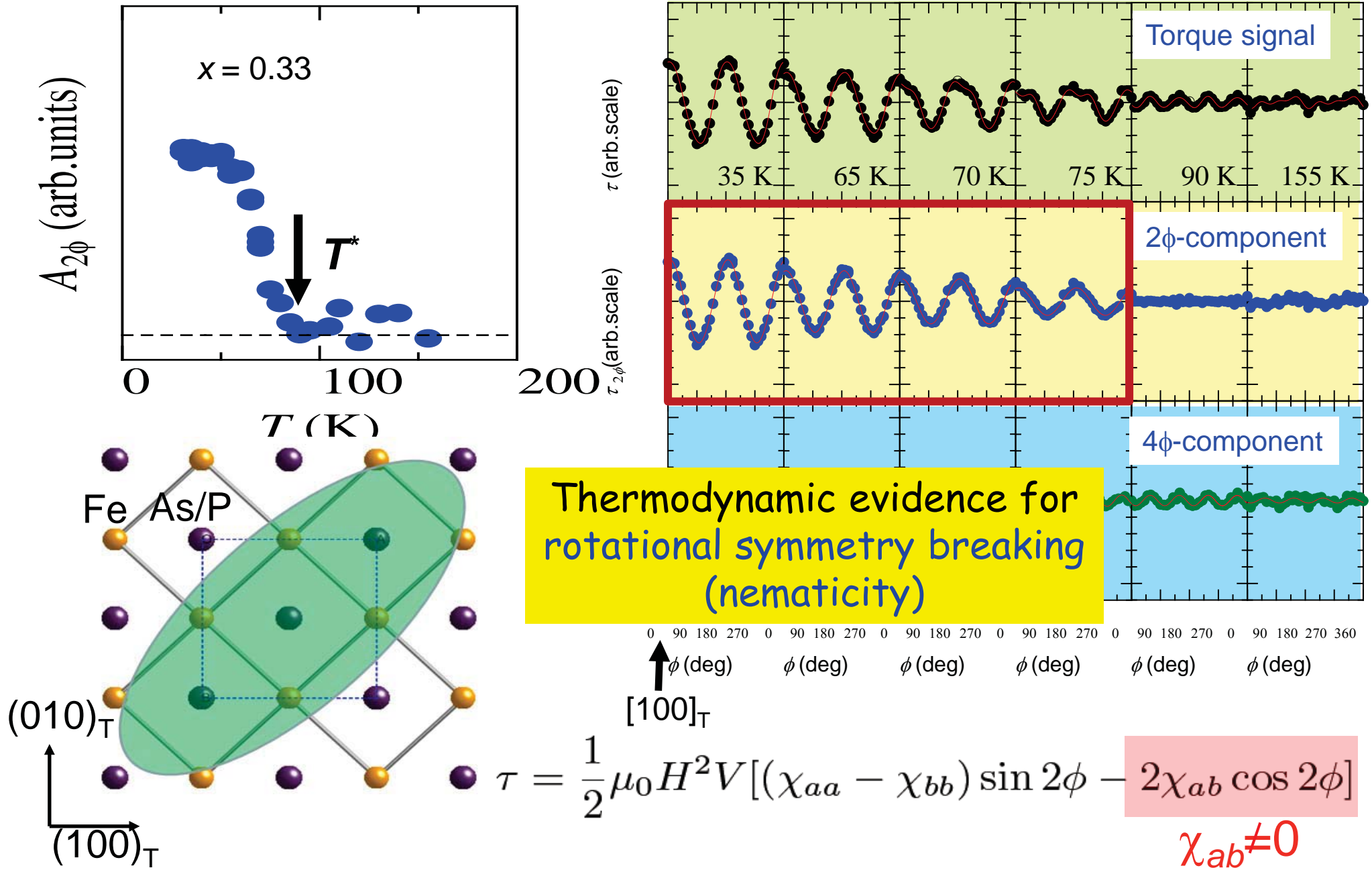
$\chi_{aa} \neq \chi_{bb}$ and/or $\chi_{ab} \neq 0$

In-plane torque magnetometry



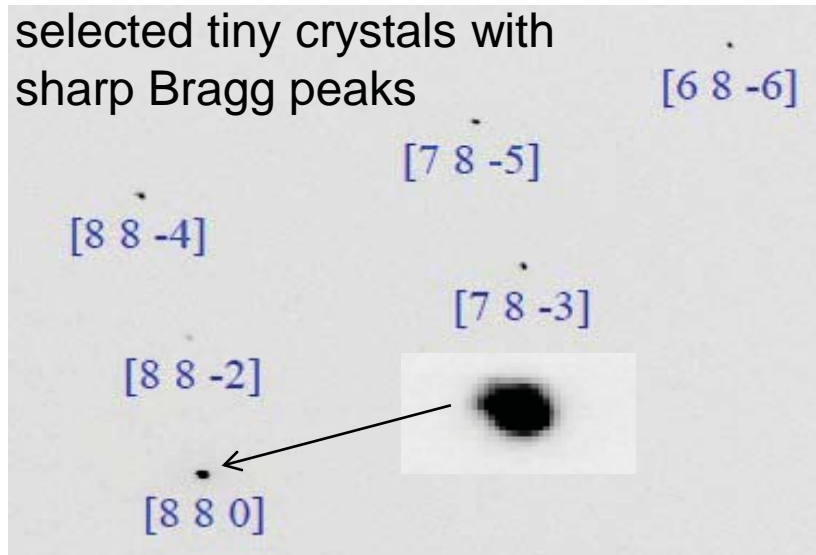
• **2 ϕ component at low temperatures**

In-plane torque magnetometry

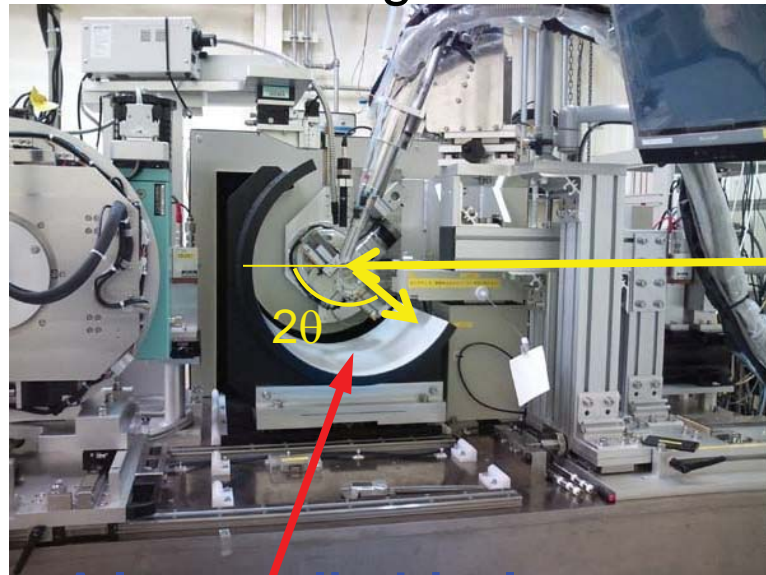


Synchrotron XRD: Detection of a tiny lattice distortion

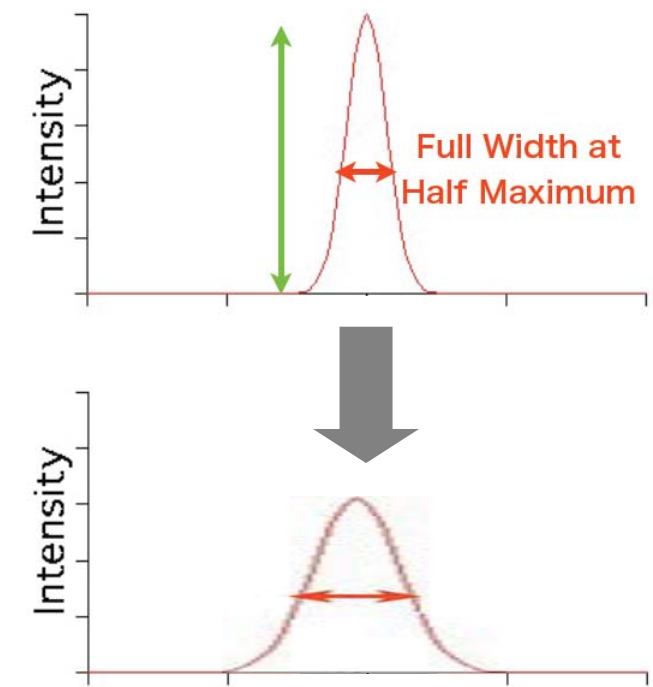
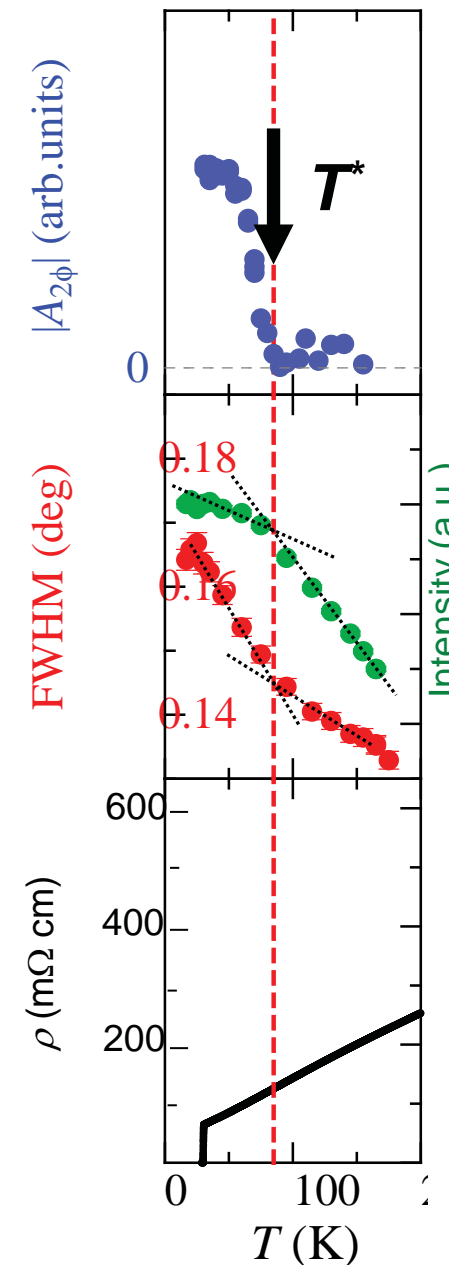
selected tiny crystals with sharp Bragg peaks



BL02B1/SPring-8



A large cylindrical imaging-plate camera



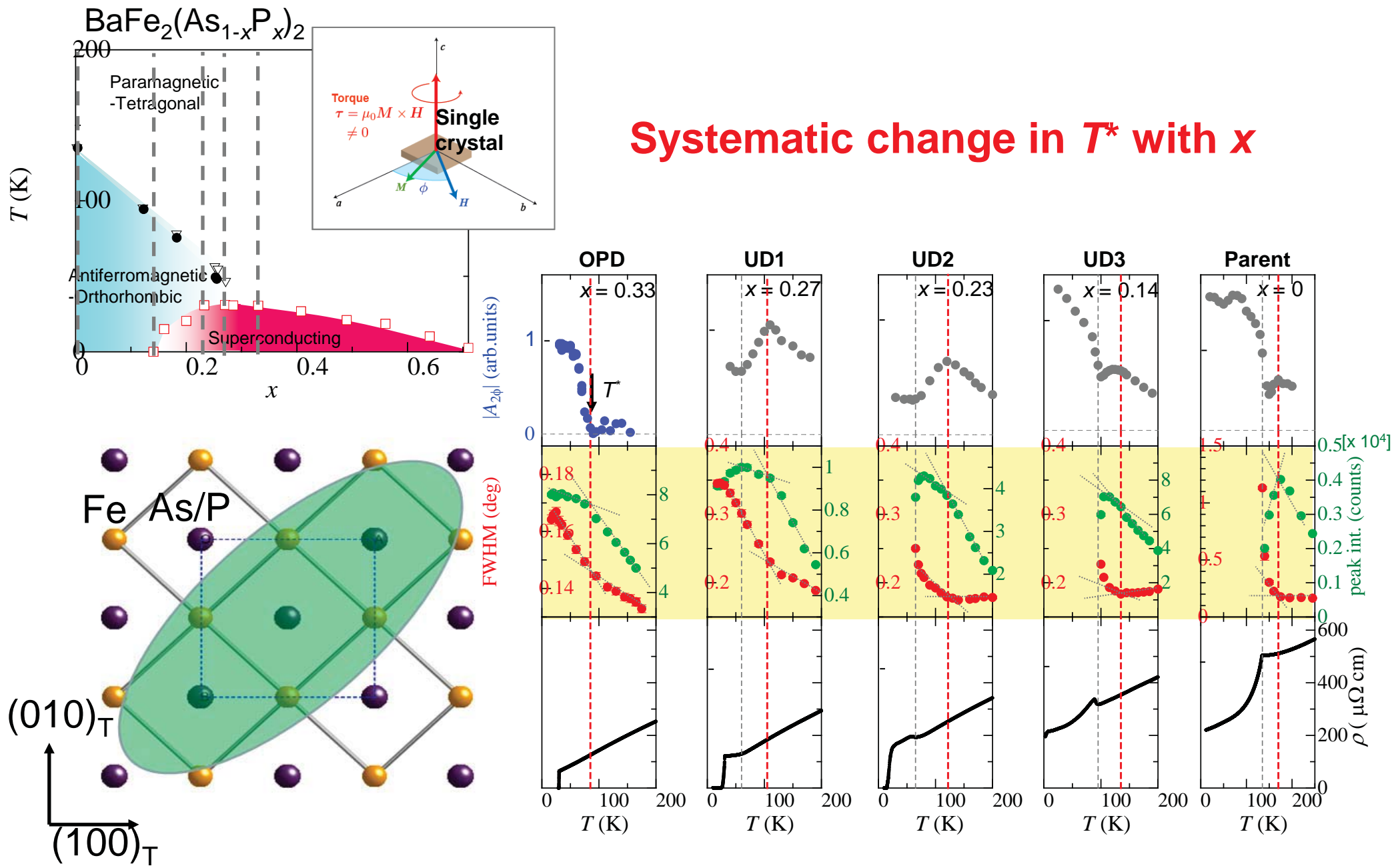
Broadening of the Bragg Peak

$(7\bar{7}0)_T$ or $(8\bar{8}0)_T$

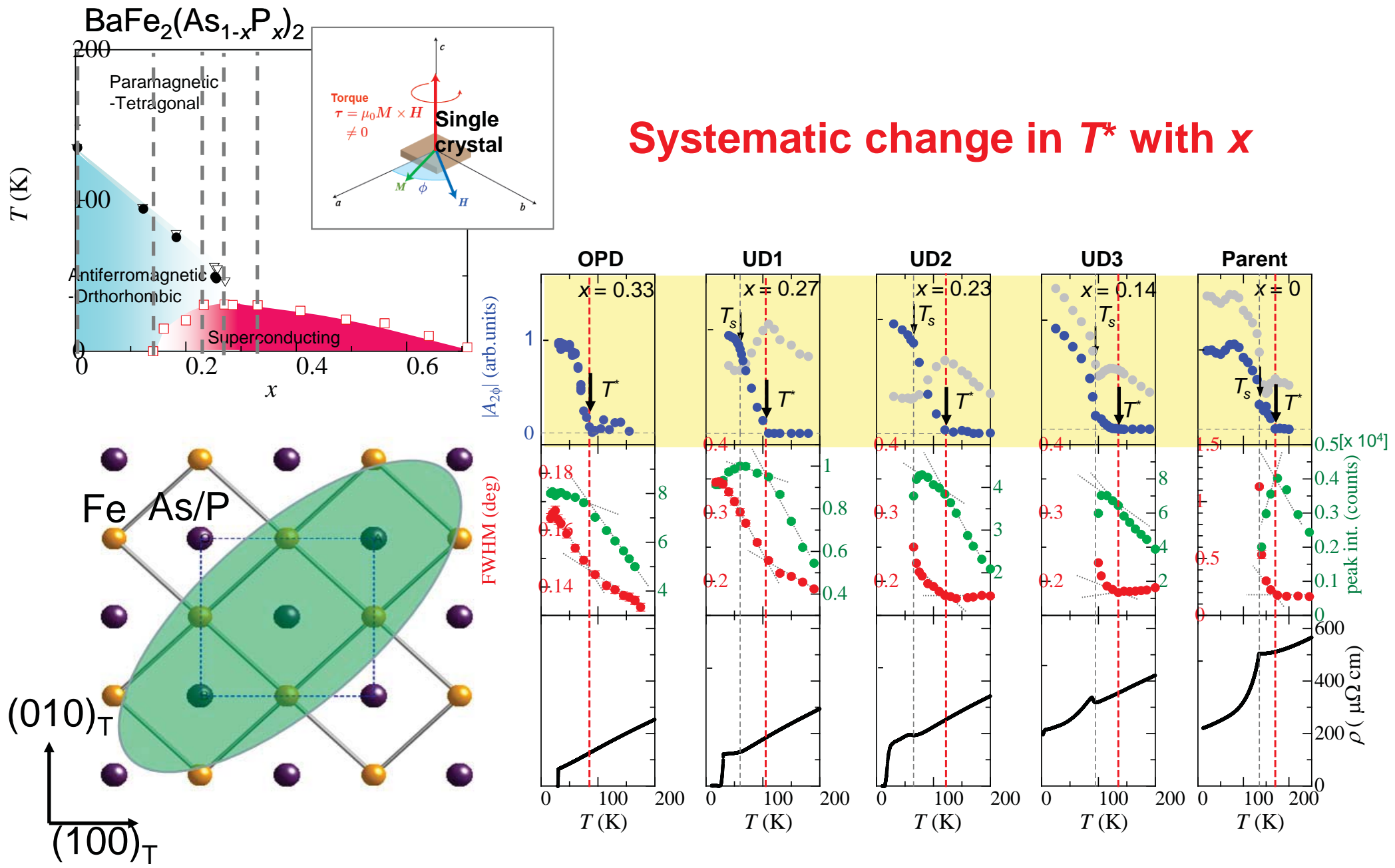
at high angle $2\theta > 120$ deg

Tiny orthorohombic distortion associated with the nematic phase transition at T^* .

Evolution with doping

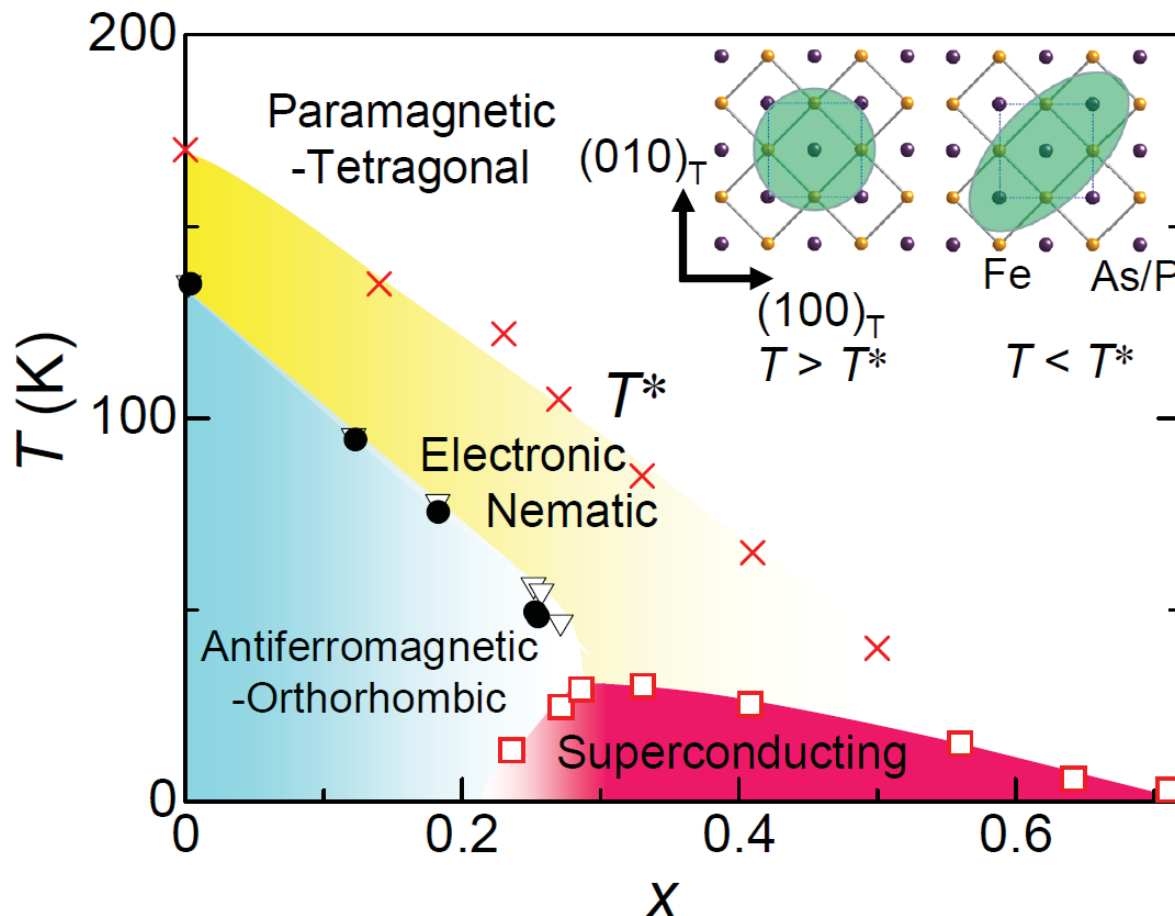


Evolution with doping



Phase diagram

S. Kasahara *et al.*, Nature **486**, 382 (2012).



Electronic nematic phase persists over a wide range of doping
Pseudogap phase ? Orbital ordering?

Optical conductivity, S. J. Moon *et al.*, PRL (2012).

Point contact spectroscopy, H. Z. Arham *et al.*, PRB (2012).

ARPES, T. Shimojima *et al.*, (unpublished).

Nematic and meta-nematic transitions

Landau free energy

$$F[\delta, \psi] = [t_s \delta^2 - u \delta^4 + v \delta^6] + [t_p \psi^2 + w \psi^4 + \mathcal{O}(\psi^6)] - g \psi \cdot \delta$$

Structural term Electronic term Coupling

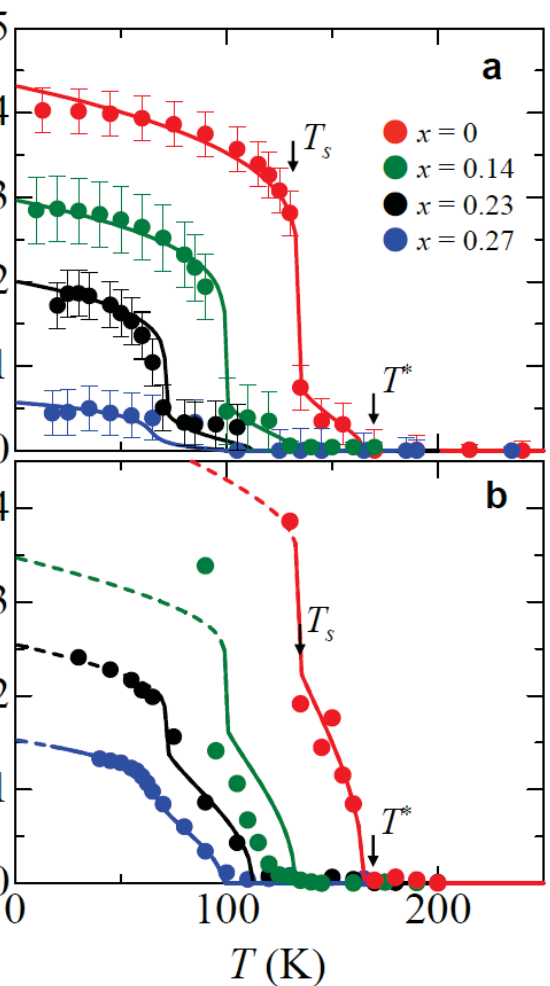
Two order parameters

$$\begin{cases} \delta = \frac{a-b}{a+b} & : \text{Orthorhombic distortion} \\ \psi \propto A_{2\phi} & : \text{Nematic order parameter} \end{cases}$$

$\left\{ \begin{array}{l} T^*: \text{Non-zero } \delta \text{ and } \psi \\ \qquad \qquad \text{Broken } C_4 \text{ symmetry} \\ T_s: \text{Finite jump of } \delta \text{ and } \psi \end{array} \right.$

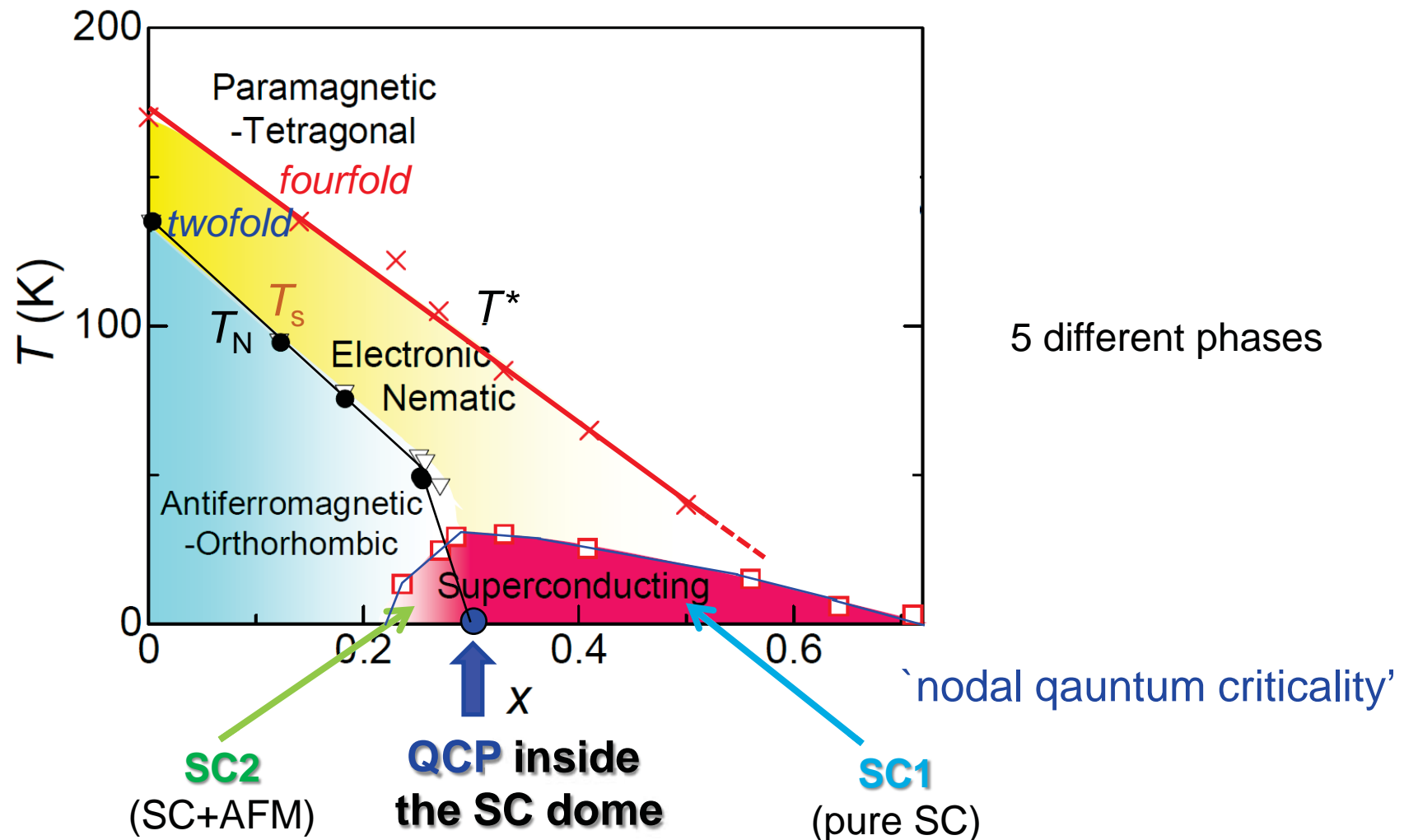
True nematic transition at T^*
‘Meta-nematic transition’ at T_s

$T^* > T_s$ implies an electronic origin of the nematic transition.



Summary: Renewed phase diagram in $\text{BaFe}_2(\text{As}_{1-x}\text{P}_x)_2$

S. Kasahara *et al.*, Nature **486**, 382 (21 June 2012).
K. Hashimoto *et al.*, Science **336**, 1554 (22 June 2012).



The nematicity appears to be a requisite for SC, and the high- T_c SC may be associated with the AF-QCP.